


 Cite this: *RSC Adv.*, 2025, 15, 35509

# Recent advances in non-conventional synthesis of N-heterocyclic compounds: emerging strategies and biological perspectives

 Niharan Sivaraj,<sup>a</sup> Kokila Sakthivel,<sup>a</sup> Kotaro Kikushima,<sup>b</sup> Marina D. Kostić,<sup>\*c</sup> Toshifumi Dohi<sup>\*b</sup> and Fateh V. Singh<sup>\*a</sup>

Nitrogen-containing heterocycles are of particular research interest as they are commonly found in naturally occurring bioactive molecules. However, traditional synthetic approaches to these compounds have various drawbacks, including slow reaction rates, harsh reaction conditions (e.g., high temperatures or strong acids), and low product yields. In recent years, non-conventional synthetic methods, such as microwave irradiation, sonochemical synthesis, and mechanochemical approaches, have emerged as efficient and sustainable alternatives. These techniques provide multiple benefits in synthetic chemistry, enabling faster reactions, enhanced product yields, and superior reaction selectivities. Moreover, they reduce the reliance on toxic solvents and lower the overall energy requirements, ultimately leading to more sustainable processes. Furthermore, the application of green chemistry principles in the synthesis of N-heterocycles has enhanced their environmental compatibility. This review focuses on recent advancements in non-conventional synthetic strategies for constructing N-heterocyclic compounds. Key scaffolds discussed include pyridines, pyrrolidines, pyrroles, imidazoles, pyrazolines, indoles, pyrazoles and 1,2,3-triazoles, along with their fused analogs. These alternative approaches are noted for their synthetic efficiency and environmentally benign nature. Furthermore, the resulting heterocycles exhibit significant potential as biologically active molecules, particularly in the context of their antimicrobial, anticancer, and antioxidant activities.

 Received 15th August 2025  
 Accepted 10th September 2025

DOI: 10.1039/d5ra06028a

[rsc.li/rsc-advances](https://rsc.li/rsc-advances)

## 1. Introduction

Heterocycles, especially those containing nitrogen atoms, are vital targets in organic synthesis. Indeed, these ring structures have garnered considerable attention due to their prevalence in numerous physiologically active compounds.<sup>1</sup> A quick analysis of the most potent pharmacophores reveals that N-heterocyclic compounds remain integral in various pharmaceutical fields.<sup>2</sup> Specifically, they act as scaffolds for molecules with significant biological properties, including antifungal, antibacterial, and anticancer drugs, as well as vitamins and herbicides. Notable examples include olaparib **1**, lclaprim **2**, clotrimazole **3**, sunitinib **4**, and ponatinib **5** (Fig. 1).<sup>3–5</sup>

To date, several methods have been developed for synthesizing heterocyclic compounds, which tend to employ expensive resources such as gold, palladium, and other costly materials,

along with catalysts that are harmful to the environment.<sup>6–13</sup> As a result, it is desirable to develop novel and more efficient approaches for the preparation of N-heterocycles using ecologically friendly, atom-economical, and inexpensive catalytic processes.

Although numerous attempts have been made to prepare N-heterocycles, conventional routes remained ineffective.<sup>14–18</sup> In

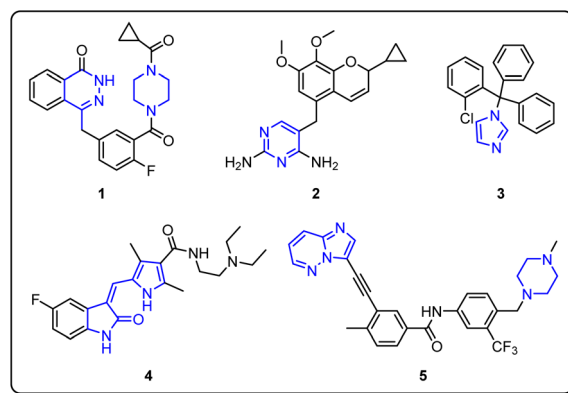


Fig. 1 Commercially available drugs containing N-heterocyclic ring systems.

<sup>a</sup>Chemistry Department, SAS, Vellore Institute of Technology – Chennai, Vandalur-Kelambakkam Road, Chennai 600127, Tamil Nadu, India. E-mail: fatehveer.singh@vit.ac.in

<sup>b</sup>College of Pharmaceutical Sciences, Ritsumeikan University, 1-1-1 Nojihigashi, Kusatsu, Shiga, Japan. E-mail: td1203@ph.ritsumei.ac.jp

<sup>c</sup>Department of Science, Institute for Information Technologies, University of Kragujevac, Jovana Cvijića bb, 34000 Kragujevac, Serbia. E-mail: mrvovic@kg.ac.rs



contrast, non-conventional approaches have been shown to provide a number of benefits over standard strategies. For example, higher yields, enhanced selectivities, and faster reaction rates have been made possible by techniques such as solvothermal synthesis,<sup>19</sup> microwave-assisted synthesis,<sup>20–25</sup> sonochemical synthesis,<sup>26–28</sup> and mechanochemical synthesis.<sup>29</sup> These techniques also frequently reduce energy consumption, employ fewer solvents, and encourage more sustainable, greener chemical processes. Thus, to overcome the drawbacks associated with traditional methods and improve both productivity and environmental compatibility, non-conventional approaches have gained popularity for the effective and environmentally benign synthesis of bioactive N-heterocycles.

This review therefore aims to highlight the contemporary use of non-conventional protocols for the synthesis of N-heterocycles with potential biological activities *via* one-pot, cycloaddition, and cyclo-condensation approaches, in addition to other modular techniques. The focus of this review is on findings published over the last decade, including the most recent studies up to 2024. Since N-heterocyclic structures exhibit a broad spectrum of biological functions, encompassing anticancer, antiviral, antibacterial, antimicrobial, antineoplastic, and anti-inflammatory effects, among others,<sup>30–34</sup> many research groups are actively developing new strategies for their preparation, as are outlined below.

### 1.1 Limitations of traditional synthetic approaches for N-heterocycles

Traditional synthetic approaches for N-heterocycles, such as the Skraup, Paal–Knorr, Fischer, Debus–Radziszewski, and Hantzsch reactions, frequently encounter multiple intrinsic drawbacks. Such protocols generally necessitate high temperatures and extended reaction durations, along with the requirement for strong acids, dehydrating substances, or oxidizing agents, ultimately resulting in competitive side reactions, low atom efficiencies, and reduced selectivities.<sup>35,36</sup> Additionally, the severe reaction conditions required by these approaches frequently limit the substrate scope, particularly when sensitive functional groups are involved, thereby reducing structural variety. In numerous instances, the employment of volatile organic solvents and hazardous chemicals additionally exacerbates the inadequate environmental compatibility and operational safety profiles of these routes.

### 1.2 Microwave-assisted synthesis

Microwave (MW) irradiation is particularly advantageous in the preparation of physiologically relevant N-heterocycles, resulting in higher yields but a lower environmental impact than conventional thermal methods.<sup>37–41</sup> Because of the homogeneous heat produced by dielectric volumetric heating during MW-assisted organic synthesis (MAOS), reactions tend to occur more quickly and selectively.<sup>42–44</sup> MW irradiation therefore provides an efficient alternative to conventional heating by directly converting electromagnetic energy into heat, revolutionizing chemistry with faster reactions and improved efficiencies. In the field of organic synthesis, MW irradiation

enables shorter reaction times and broader reaction ranges, benefiting various industries (*e.g.*, the pharmaceutical industry) by accelerating the production of novel compounds. MW heating primarily arises from dielectric polarization, where molecules align with oscillating electromagnetic fields, absorbing energy and generating heat. The efficiency of this process is measured by the dissipation factor ( $\tan \delta = \epsilon''/\epsilon'$ ), while the Maxwell–Wagner effect further contributes to an enhanced efficiency in heterogeneous systems.<sup>45</sup> Polar solvents, such as water, methanol, and acetone efficiently absorb MW irradiation, whereas non-polar solvents, such as hexane and toluene, do not. MW energy, as a type of non-ionizing radiation, induces ion migration and dipole rotation without altering molecular structures.<sup>46</sup> Molecules therefore attempt to align with the applied field, generating friction and heat. Upon field removal, thermal agitation restores disorder, thereby releasing energy.<sup>47</sup> This internal heating is more uniform than that achieved using conventional methods, thereby minimizing temperature gradients in the reaction systems.

MW-assisted reactions demonstrate significant advantages in terms of the reaction speed, efficiency, and selectivity. The effectiveness of a MW-assisted reaction largely depends on the ability of the reaction mixture to absorb MW energy, which is influenced by the choice of solvent and its loss tangent ( $\delta$ ), as detailed above. Consequently, solvents can be classified as high, medium, or low MW absorbers, and mixed solvents can be used to tune this property based on the desired reaction system. Furthermore, advancements in MW reactor technologies, particularly silicon carbide reaction vessels and fiber optic temperature probes, have facilitated accurate temperature measurements and a clearer distinction between MW-induced and conventional thermal effects.

Commonly utilized systems include the CEM Discover SP, Biotage Initiator+, Anton Paar Monowave 400, and Milestone Ethos EASY, all of which are designed for safe and efficient chemical synthesis. These reactors can handle reaction scales ranging from a few milligrams to 30–100 grams, depending on the vessel type and system configuration. Method development often involves smaller scales (5–100 mg), while multi-vessel or batch systems facilitate medium scale (0.1–5 g) and larger scale (up to ~100 g) processes.

### 1.3 Sonochemical synthesis

The application of ultrasonic irradiation represents a new field of study that employs waves with frequencies ranging between 20 kHz and 1 MHz.<sup>48,49</sup> The use of ultrasound technology in organic synthesis is therefore growing and is particularly crucial in the field of green chemistry. The effects observed under ultrasonic conditions are attributed to cavitation, which is a physical process wherein vaporous and gaseous cavities form, expand, and collapse in the irradiated liquid. High local temperatures and pressures are produced as a result, thereby promoting mass transfer and causing turbulent flow. In organic synthesis, ultrasonication has emerged as a useful method, especially for multicomponent reactions, which render it possible to efficiently synthesize complicated organic molecules



from easily accessible starting materials.<sup>50–55</sup> Indeed, the sonochemical synthesis of heterocycles has gained significant attention among both organic and medicinal chemists worldwide. This technique accelerates reactions by increasing product yields, reducing reaction times, and improving reaction selectivities. Unlike conventional methods, ultrasound synthesis is straightforward, cost-effective, and widely accessible. Additionally, it often eliminates the requirement for external heating, as the ultrasonic waves themselves act as catalysts, ultimately boosting the reaction rate.

#### 1.4 Mechanochemical synthesis

Mechanochemical techniques are becoming more widely adopted as greener synthetic methods in response to the need for safer and cleaner chemical processes. While the significance of solvents in the extraction and purification steps remains crucial, mechanochemical techniques have been demonstrated to promote reactant interactions while improving the extent of reaction control and temperature management. The potential value in reducing solvent usage has also been recognized. Ball milling represents a frequently used technique in mechanochemistry, wherein mechanical forces (*e.g.*, compression and friction) promote the reactions, and energy is transferred through impact and shear forces. These conditions enable intimate mixing, increased surface contact, and localized heating, thereby facilitating bond formation and cleavage in the absence of bulk solvents. The regulated, contained conditions provided by modern shaker and planetary mills ensure more consistent results than traditional manual grinding, which is subject to human and environmental variability. Additionally, mechanochemistry can allow reaction pathways to be modified by allowing access to high-energy intermediates and non-classical transition states that would otherwise be inaccessible under conventional conditions. Furthermore, the absence of solvent dielectric effects and temperature control frequently produces distinct reactivity profiles and polymorph results, particularly in co-crystal and supramolecular syntheses.<sup>29</sup>

Commonly utilized equipment includes the Retsch PM100 and PM400 planetary mills, the Retsch MM400 mixing mill, and the Fritsch Pulverisette 7 planetary micro mill, all of which can operate at varied speeds and accommodate different jar sizes (10–500 mL). These mills can handle reaction scales ranging from a few tens of milligrams to several tens of grams, depending on the jar volume and ball-to-powder ratio. The reactions are carried out in jars constructed of stainless steel, zirconia, agate, or tungsten carbide, generally under ambient or inert atmospheres.

#### 1.5 Solvothermal synthesis

The solution-based synthetic approach known as solvothermal synthesis entails conducting chemical reactions in a closed system at high pressures and temperatures, usually above the standard boiling point of the solvent. Metal oxides, metal chalcogenides, coordination complexes, metal–organic frameworks, and other functional nanostructures<sup>56,57</sup> are among some the crystalline materials that are commonly prepared using this

technique. Solvothermal circumstances create a particular high-temperature, high-pressure environment that improves the precursor solubility, accelerates the reaction kinetics, and permits regulated nucleation and crystal formation processes. The nature of the solvent, including its polarity, coordinating ability, and dielectric constant, plays a critical role in directing the morphology, size, and phase of the resulting product. Moreover, solvothermal synthesis provides access to metastable phases and complex architectures that are often unattainable under ambient or conventional thermal conditions.<sup>19</sup>

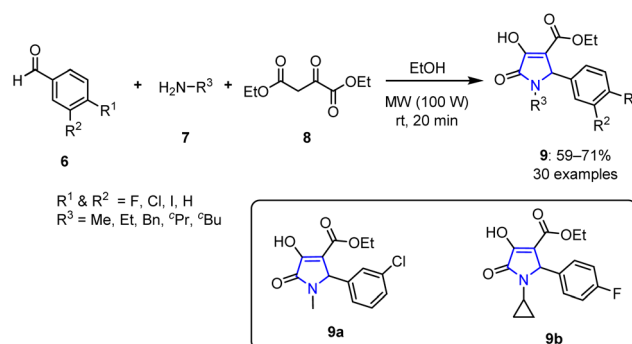
Solvothermal techniques are particularly useful in the preparation of bioactive heterocycles because they are more efficient and selective than traditional synthetic approaches. Furthermore, these methods can reduce energy consumption and lower solvent volumes, rendering them more sustainable and greener options.<sup>58,59</sup>

## 2. N-heterocycles with anticancer activity

Anticancer molecules are compounds that inhibit or destroy cancer cells by targeting specific cellular pathways. They work through various mechanisms, including DNA intercalation, enzyme inhibition, apoptosis induction, and angiogenesis suppression. Common classes include alkaloids, flavonoids, terpenoids, and N-heterocycles, as well as synthetic agents such as tyrosine kinase inhibitors and platinum-based drugs. These molecules form the basis of chemotherapy, immunotherapy and targeted cancer treatments.<sup>60–62</sup>

### 2.1 Microwave-assisted synthesis of anticancer agents

**2.1.1 Pyrrole.** Numerous traditional methods exist for synthesizing pyrroles, including the Knorr, Paal–Knorr, Hantzsch condensation, and Clauson–Kaas reactions. However, when carried out using conventional heating approaches, these methods often demand harsh reaction and work-up conditions, which can negatively affect the product yields. In contrast, newer protocols utilizing MW irradiation offer significant improvements in the efficiency of such reactions. For example, in 2018, Manta *et al.* carried out a multicomponent reaction using equimolar amounts of aromatic aldehydes **6**, primary



Scheme 1 MW-assisted synthesis of various new 3-hydroxy-3-pyrroline-2-ones **9**.



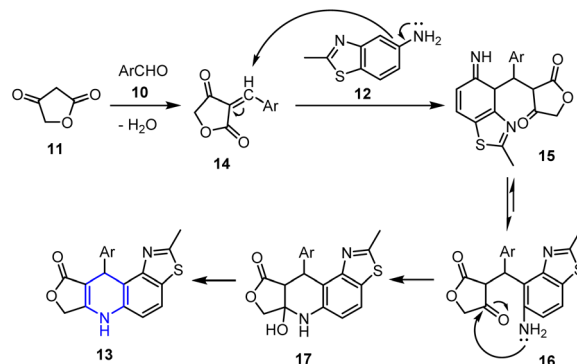
amines **7**, and diethyl oxalacetate **8** in ethanol under 100 WMW irradiation for 20 min to yield various new 3-hydroxy-3-pyrrolin-2-ones **9** in moderate yields 59–71% (Scheme 1).<sup>63</sup>

Among the various synthesized compounds, **9a** demonstrated the most promising activity against leukemia cells. Additionally, pyrrole derivatives bearing cyclobutyl substituents exhibited increased efficacies against cervical carcinoma and leukemia, particularly when paired with halogen atoms such as chlorine or iodine (*cf.*, fluorine). *para*-Substitution with a chlorine atom further enhanced the activities of these compounds, particularly in instances of double aromatic substitution. Moreover, the newly synthesized pyrrole-based compound **9b** displayed antiviral effects against the yellow fever virus.

**2.1.2 Piperidine.** The MW-assisted synthesis of piperidines offers faster reactions, higher yields, and improved selectivities under milder reaction conditions. In this context, Shi *et al.* prepared 4-aza-podophyllotoxin analogues **13** in good yields 70–83% *via* a three-component process under MW irradiation (at 150 W). These reactions were performed using various substituted aromatic aldehydes **10** in combination with tetronic acid **11** and benzothiazole **12** (Scheme 2).<sup>64</sup>

The proposed mechanism for the above transformation (see Scheme 3) begins with a Knoevenagel condensation between aldehyde **10** and tetronic acid **11**, forming a  $\beta,\gamma$ -unsaturated intermediate **14**. This is followed by the Michael addition of 2-methylbenzo[*d*]thiazol-5-amine **12** to intermediate **14**, yielding an open-chain intermediate **16** *via* addition product **15**. Finally, intramolecular cyclization and dehydration from **17** produce the final N-heterocyclic product **13**.

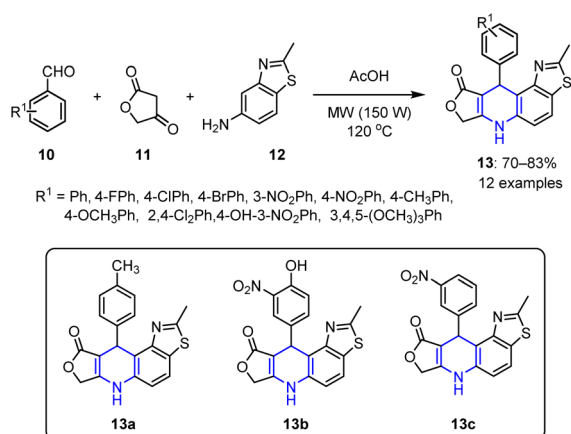
All synthesized 4-aza-podophyllotoxin analogues **13** demonstrated good cytotoxicities against different cell lines. Specifically, compound **13a**, which possesses a  $-\text{CH}_3$  substituent at the *para*-position of the aromatic ring, exhibited the highest cytotoxicity against the MCF-7 breast cancer cell line, with an  $\text{IC}_{50}$  value of  $25.68 \mu\text{g mL}^{-1}$ . Conversely, compound **13b**, bearing nitro and hydroxyl substituents, showed the strongest cytotoxic effects across three cell lines, namely the MCF-7 breast cancer cell line ( $\text{IC}_{50} = 56 \mu\text{g mL}^{-1}$ ), the M14 malignant melanoma cell



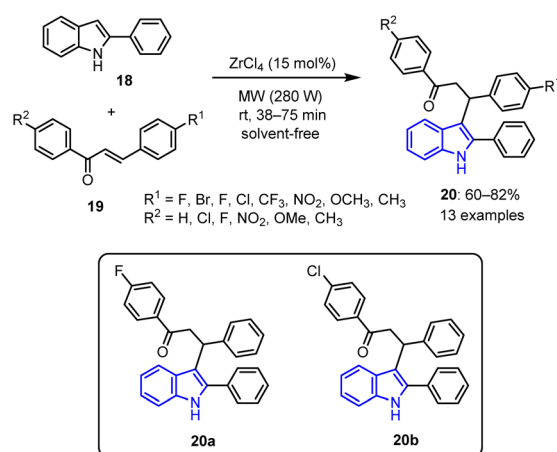
Scheme 3 Proposed mechanism for the synthesis of 4-aza-podophyllotoxin analogs **13**.

line ( $\text{IC}_{50} = 33.9 \mu\text{g mL}^{-1}$ ), and the SW1116 colon carcinoma cell line ( $\text{IC}_{50} = 69.4 \mu\text{g mL}^{-1}$ ). Additionally, compound **13c**, bearing a nitro substituent, demonstrated a significant inhibitory effect against SW1116 colon carcinoma cells, with an  $\text{IC}_{50}$  value of  $25.98 \mu\text{g mL}^{-1}$ . Notably, both compounds **13b** and **13c** contain *meta*-nitro groups on their aromatic rings, suggesting that this functionality may enhance their cytotoxic effects.

**2.1.3 Indole.** Indole is a key heterocyclic scaffold with a versatile reactivity and strong biological relevance. Its structure enables facile functionalization, rendering it of particular importance in drug design, with its derivatives showing diverse pharmacological activities. In this context, Tarun *et al.* detailed the synthesis of 3-(3-oxoaryl) indole derivatives **20**<sup>65</sup> *via* a Michael addition reaction, wherein 2-phenylindole **18** reacts with a range of chalcones **19**. This approach employs  $\text{ZrCl}_4$  as a relatively non-toxic catalyst and is carried out under MW-promoted solvent-free conditions. The reaction yields ranged from 60% to 82%, as detailed in Scheme 4. Notably, the use of



Scheme 2 Synthetic protocol for the preparation of 4-aza-podophyllotoxin analogs **13**.



Method	Solvent	Reaction time	Yield
Conventional heating (reflux)	MeCN	8 h	73%
MW (280 W, rt)	Solvent-free	40 mins	91%

Scheme 4 Synthesis of 3-(3-oxoaryl) indole derivatives **20**.

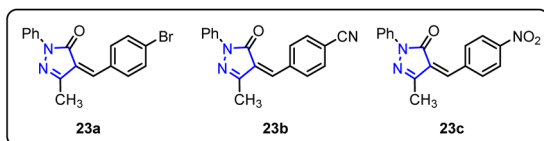
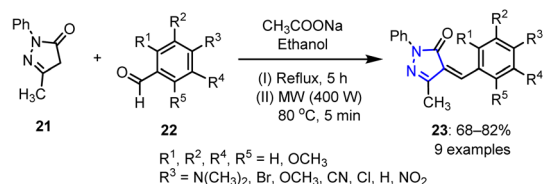


MW irradiation produced an efficient reaction system for accomplishing quick and effective chemical transformations with excellent selectivities and yields.

Among the synthesized indole derivatives, compounds **20a** and **20b** demonstrated effectiveness in inhibiting the growth of the murine melanoma B16F10 cancer cell line along with the MCF-7 human breast cancer cell line, exhibiting maximum  $IC_{50}$  values in the range of 10–15  $\mu\text{M}$ . Furthermore, molecular docking studies revealed that compounds **20a** and **20b** exhibit high docking affinities with the colchicine binding site of the tubulin receptor (10.4 and 9.9  $\text{kcal mol}^{-1}$ , respectively). These results demonstrate the exceptional potential of compounds **20a** and **20b** for use as anticancer drugs to inhibit tubulin *via* contact with the colchicine binding site.

**2.1.4 Pyrazole.** The MW-assisted synthesis of pyrazoles enables rapid, high-yielding reactions with improved purities under mild and eco-friendly conditions. Common routes to pyrazoles include the cyclocondensation of hydrazines with 1,3-dicarbonyl compounds or enones, thereby rendering MW irradiation a valuable tool for efficient pyrazole synthesis in medicinal chemistry. In this context, Shroff *et al.* reported the synthesis of pyrazole derivatives through a novel method,<sup>66</sup> wherein 3-methyl-1-phenyl-1*H*-pyrazol-5(4*H*)-one **21** was reacted with various substituted aryl aldehydes **22** in the presence of anhydrous sodium acetate and ethanol. MW irradiation was subsequently performed at 400 W and 80 °C for 5 min to produce the desired arylidene derivatives **23** in moderate yields (68–82%), as depicted in Scheme 5.

Among the synthesized arylidene derivatives, compounds **23a**, **23b**, and **23c** demonstrated significant anti-proliferative effects against various cancer cell lines, with  $IC_{50}$  values ranging from 2 to 7  $\mu\text{M}$ . Notably, compound **23c** proved to be the most potent anticancer compound. Although this



Compound	Reaction time		Yield	
	Conventional heating (reflux)	MW	Conventional heating (reflux)	MW
<b>23a</b>	5 h	5 min	69%	78%
<b>23b</b>	5 h	5 min	80%	84%
<b>23c</b>	5 h	5 min	78%	84%

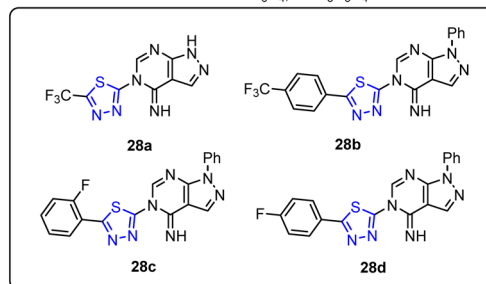
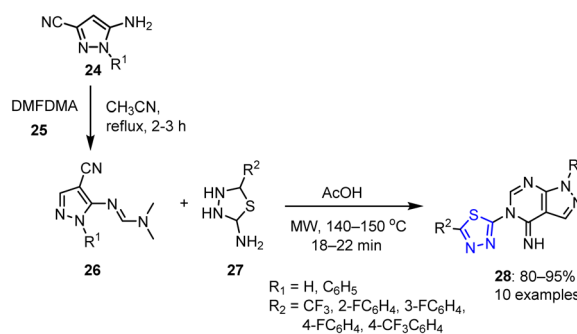
Scheme 5 Synthetic route to functionalized 4-arylidene-3-methyl-1-phenyl-1*H*-pyrazol-5(4*H*)-one derivatives **23**.

compound had no effect on tubulin polymerization, it effectively induced apoptosis in drug-resistant cancer cells by increasing the expression of mitochondria-dependent pro-apoptotic markers, namely Bax and caspase-3. This compound therefore demonstrates an encouraging anticancer activity, wherein it induces cancer cell death by interacting with the mitochondria.

**2.1.5 Thiadiazole.** Song *et al.* reported the reaction of amino pyrazoles **24** and *N,N*-dimethyl formamide dimethyl acetal (DMFDMA) **25** in the presence of acetonitrile to yield the corresponding amidines **26**.<sup>67</sup> Subsequent cyclocondensation with suitable substituted-1,3,4-thiadiazole derivatives **27** in acetic acid under MW irradiation yielded a novel series of pyrazolo pyrimidine derivatives **28** incorporating 1,3,4-thiadiazole moieties in yields of 80–95% (Scheme 6).

It was demonstrated that when a hydrogen atom (*cf.*, a phenyl substituent) occupies the  $R^1$  position of the pyrazole ring, these compounds exhibited significantly greater anti-cancer activities. Additionally, compounds bearing trifluoromethyl **28a**, 4-trifluoromethyl benzene **28b**, 2-fluorobenzene **28c**, and 4-fluorobenzene **28d** substituents also exhibited strong anticancer activities against human leukemia cells (HL-60). Specifically, compounds **28a** and **28b** were found to be more effective than doxorubicin. Notably, the addition of a  $\text{CF}_3$  group led to a significantly enhanced biological activity.

**2.1.6 Imidazole.** Conventional routes to imidazole typically require prolonged heating, strong acids, or dehydrating agents, and often result in moderate yields along with side product



Method	Compound	Reaction time	Yield
Conventional heating (118°C)	<b>28a</b>	6 h	88%
MW	<b>28a</b>	18 min	85%

Scheme 6 Synthetic protocol to functionalized pyrazolo pyrimidines **28** bearing 1,3,4-thiadiazole moieties.



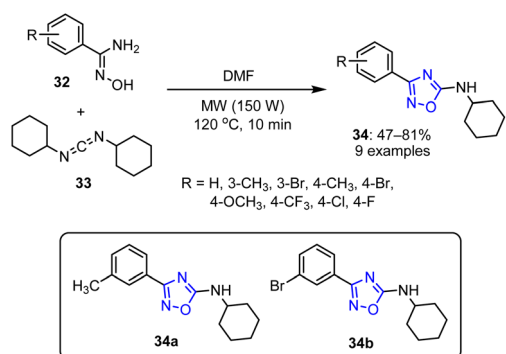


Scheme 7 Synthesis of imidazo[4,5-*f*]-1,10-phenanthroline derivatives **31** under MW irradiation.

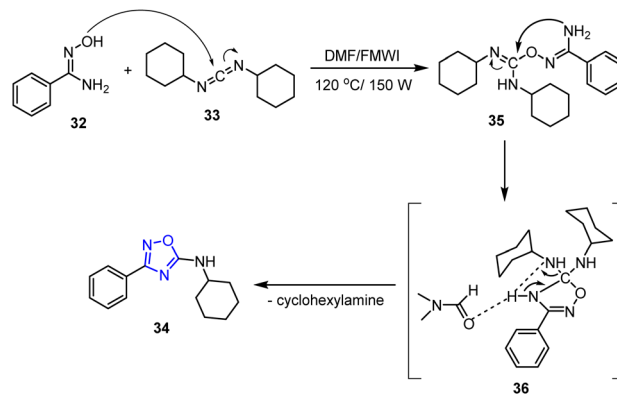
formation. MW-assisted synthesis overcomes these limitations by enabling rapid, uniform heating, thereby reducing reaction times, improving yields and selectivities, and allowing solvent-free or greener conditions to be employed. Imidazoles are efficiently synthesized *via* the Debus–Radziszewski condensation of a 1,2-dicarbonyl compound and an aldehyde in the presence of ammonium acetate. This simple, versatile method often employs ethanol or acetic acid, and can be accelerated by MW irradiation to give higher yields and shorter reaction times. In 2017, Zheng *et al.* investigated the reactions between phendione **29** and various aromatic aldehydes **30** in the presence of glacial acetic acid and ammonium acetate under MW irradiation.<sup>68</sup> As a result, various phenanthroimidazole derivatives **31** were obtained in excellent yields of 82–95% (Scheme 7).

The synthesized phenanthroimidazole derivatives **31** were found to effectively inhibit the formation and proliferation of human hepatocarcinoma SMMC7721 cells, human lung adenocarcinoma A549 cells, and human colorectal carcinoma SW620 cells. The maximum inhibitory activity of **31** was an  $IC_{50}$  15.03  $\mu$ M, with a reduced toxicity being observed against normal cells. Further research showed that the nitro-substituted compound could disperse in the mitochondria of A549 cells, triggering cell death by G1 phase arrest. Furthermore, it showed a moderate affinity for binding to the Bcl-2 G-quadruplex DNA. These compounds also showed potential inhibitory effects against tumor cell development.

**2.1.7 Oxadiazole.** In 2018, a study by Oliveira *et al.* investigated the reaction of aryl amidoximes **32** with *N,N*-dicyclohexylcarbodiimide (DCC) **33** under MW irradiation at 150 W in DMF.<sup>69</sup> This methodology afforded 1,2,4-oxadiazole derivatives **34** in moderate-to-good efficiencies, achieving yields between 47% and 81% (Scheme 8).



Scheme 8 Synthesis of *N*-cyclohexyl-1,2,4-oxadiazole derivatives **34**.



Scheme 9 Plausible reaction pathway for the synthesis of 1,2,4-oxadiazole derivatives **34**.

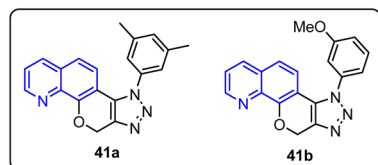
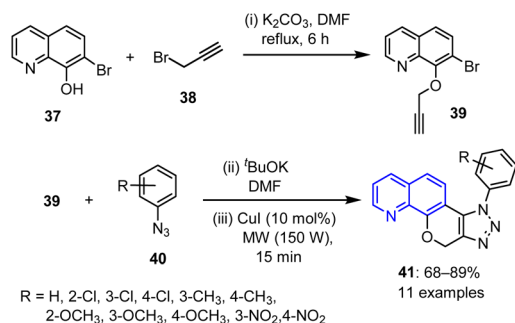
The proposed reaction mechanism begins with the nucleophilic attack of benzamidoxime **32** on DCC, forming intermediate **35**. The reaction proceeds through a transition state **36**, and is accelerated by DMF due to its high dielectric constant, which renders this solvent more reactive under MW irradiation. Solvent-facilitated proton transfer then leads to the elimination of cyclohexylamine, yielding the final product **34** (Scheme 9).

The cytotoxic activities of the samples were subsequently evaluated using the MTT assay. Specifically, they were tested at concentrations of 100  $\mu$ M for HCT-116 cells and 25  $\mu$ M for the other cell lines. After dilution in the culture media, the compounds were added to each well, and the MTT assay was employed to determine the  $IC_{50}$  values of the active compounds against the B16F10, SNB-19, PC-3, HCT-116, and L929 cell lines after incubation for 72 h. Among the synthesized compounds, *meta*-substituted compounds **34a** and **34b** showed the most promising anticancer effects, with  $IC_{50}$  values of 13.62 mM against SNB-19 and 21.74 mM against PC-3.

**2.1.8 Quinolines.** Traditional synthetic approaches to quinoline, such as the Skraup and Friedländer reactions, often require strong acids, high temperatures, and extended durations, resulting in safety issues and limited efficiencies. MW-assisted synthesis offers a technically superior alternative by providing rapid thermal activation, enhanced yields, reduced reaction times, and improved functional group tolerances under milder and often solvent-free conditions. In this context, Babu *et al.* prepared emergent fused triazolyl pyranoquinolines **41** *via* a three-stage process (Scheme 10).<sup>70</sup> Initially, 7-bromoquinolin-8-ol **37** was treated with  $K_2CO_3$  in DMF, followed by the addition of propargyl bromide **38**. After heating the resulting mixture under reflux for 6 h, 7-bromo-8-(prop-2-ynyloxy)quinoline **39** was obtained. Subsequently, intermediate **39** was treated with aryl azide **40**,  $t$ BuOK, and DMF, prior to a subsequent reaction with copper iodide under MW irradiation to produce [1,2,3]triazolo-pyrano[3,2-*h*] quinolines **41** in yields of 68–89%.

The cytotoxic activities of the synthesized compounds were subsequently tested against the alveolar carcinoma (A-549), breast carcinoma (MCF-7), and cervical carcinoma (HeLa) cell lines. Compound **41a**, bearing a dimethyl phenyl substituent,





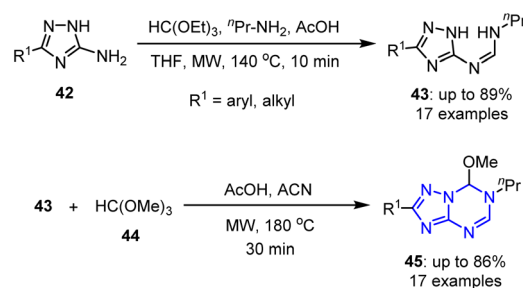
Method	Solvent	Reaction time	Yield
Conventional heating (140 °C)	DMF	24 h	upto 58%
MW	DMF	15-20 min	74-78%

Scheme 10 Synthetic route to fused triazolyl pyranoquinolines 41.

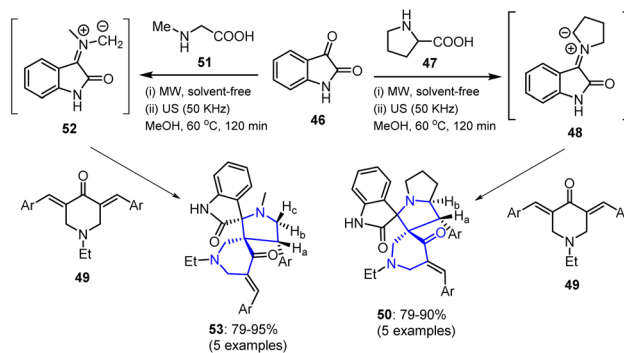
showed a strong activity against HeLa and MCF-7 cells, with IC<sub>50</sub> values of 11.42 ± 0.6 and 16.88 ± 0.5 μM, respectively. Additionally, compound **41b**, bearing a benzyloxy substituent on its triazole ring showed a moderate activity, with IC<sub>50</sub> values of 15.67 ± 0.6 and 31.44 ± 0.5 μM against the HeLa and MCF-7 cell lines, respectively. Alkyl and alkoxy substituents on the triazole ring also led to enhanced activities. In contrast, electron-withdrawing substituents, such as chloro and nitro groups, exhibited fair-to-inadequate efficacies against all three cell lines.

**2.1.9 Azapurines.** Alena *et al.* reported the MW-assisted synthesis of novel 6-methoxy-5,6-dihydro-5-azapurines **45**, which possess a purine-like framework and demonstrate potential applications in drug discovery.<sup>71</sup> This rapid and straightforward protocol employs easily accessible reagents, such as trimethyl orthoformate **44**, acetic acid, and *N,N*-disubstituted formamides **43** derived from 1,2,4-triazol-5-amines **42**.<sup>72–75</sup> Biological evaluations revealed that certain compounds decreased the viabilities of HepG2 (liver) and A549 (lung) cancer cell lines in a dose-dependent fashion, while showing minimal interactions with five purinergic receptors. These results highlight their selective anticancer activities and underscore their potential as promising candidates for further drug development (Scheme 11).

**2.1.10 Oxindole.** Spirocyclic bioactive N-heterocycles are a unique class of compounds featuring a spiro junction wherein two rings share a single atom. The incorporation of nitrogen into the ring system enhances their biological activities, rendering them valuable scaffolds in the field of drug discovery.<sup>76–78</sup> In this context, Dina *et al.* synthesized novel spiropyrrolizine **50** and pyrrolidineoxindole **53** derivatives *via* the chemo- and regioselective reaction of bis[arylmethylidene]



Scheme 11 MW-assisted synthetic methodology for the preparation of 6-methoxy-5,6-dihydro-5-azapurines 45.

Scheme 12 Synthesis of spiropyrrolizine **50** and pyrrolidineoxindole **53** derivatives.

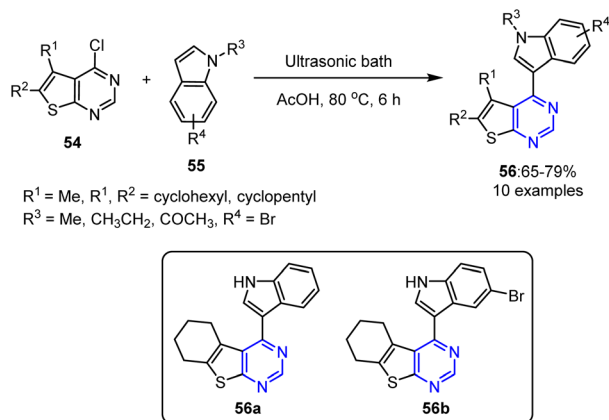
piperidin-4-ones **49**, isatin **46**, and either L-proline **47** or sarcosine **51** (Scheme 12).<sup>79</sup> The reaction was performed under conventional, ultrasonic, and MW-assisted conditions, resulting in efficient product formation through **48** or **52** as an intermediate. The resulting derivatives were evaluated for their antitumor activities against MCF-7 (breast cancer) and HepG2 (liver cancer) cell lines.

## 2.2 Sonochemical synthesis of anticancer agents

**2.2.1 Pyrimidine.** A sonochemical approach was employed by Sowmy *et al.* to prepare 4-(1*H*-indol-3-yl)thieno[2,3-*d*]pyrimidines **56** through the heteroarylation of 4-chloro-thieno[2,3-*d*]pyrimidines **54** with diverse indoles **55**.<sup>80</sup> The reaction, which was promoted by acetic acid (AcOH) as both a solvent and a catalyst, yielded the desired products in good yields. This metal-free strategy offers benefits such as straightforward conditions, a faster reaction time, and green energy utilization. Nevertheless, the technique failed with *N*-acetyl indole, demonstrating a key limitation (Scheme 13).

This reaction began with the ultrasound-promoted protonation of the azomethine nitrogen atom in chlorinated substrate **54**, generating resonance-stabilized intermediate **57**. The resulting partial positive charge on the chlorine-bonded carbon atom facilitated nucleophilic attack by the C-3 position of indole **55**, producing adduct **58**. The elimination of HCl *via* intermediates **59** and **60** resulted in the formation of the target 4-(1*H*-indol-3-yl)thieno[2,3-*d*]pyrimidine derivatives **56**. This reaction worked efficiently under open air and nitrogen



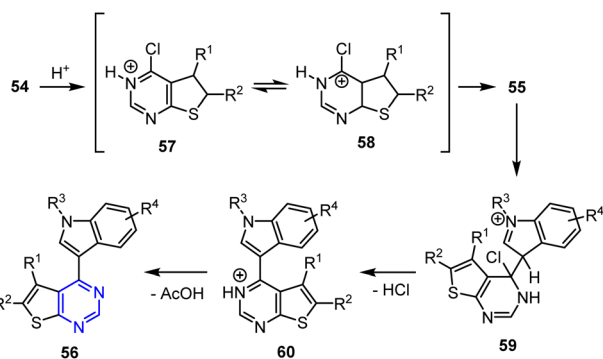


Scheme 13 Sonochemical synthesis of 4-(1H-indol-3-yl)thieno[2,3-d]pyrimidine derivatives **56**.

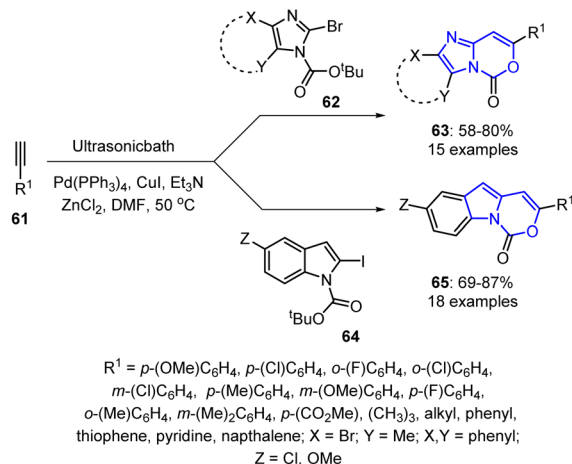
atmospheres, ruling out the involvement of a radical mechanism (Scheme 14).

The newly synthesized thieno[2,3-*d*] pyrimidine derivatives **56** were assessed for their TNF- $\alpha$  inhibition abilities *in vitro* (10  $\mu\text{M}$ ), using rolipram and thalidomide as positive controls. Among the tested derivatives, compounds **56a** and **56b** exhibited  $79.3 \pm 2.8\%$  and  $71.5 \pm 1.2\%$  TNF- $\alpha$  inhibition, respectively, compared to  $96.3 \pm 0.7\%$  for rolipram (at 10  $\mu\text{M}$ ) and  $63.9 \pm 3.9\%$  for thalidomide (200  $\mu\text{M}$ ). Consequently, compounds **56a** and **56b** emerged as viable lead molecules, showing greater TNF- $\alpha$  inhibitory activities than thalidomide despite being less potent than rolipram.

Additionally, Venkata *et al.* reported a sonochemical approach toward oxazinone derivatives **63** and **65** using Pd/Cu catalysts and  $\text{ZnCl}_2$ . This reaction involved coupling 2-iodoindole derivatives **62** and **64** with numerous terminal alkynes **61** in the presence of  $(\text{PPh}_3)_4\text{Pd}$ , CuI, and  $\text{ZnCl}_2$  in DMF under ultrasonic irradiation.<sup>81,82</sup> The reaction proceeded *via* a cascade pathway involving C-C coupling followed by intramolecular cyclization in a regioselective manner, yielding the target compounds in good-to-acceptable yields. This methodology offers advantages such as mild reaction conditions, shorter



Scheme 14 Sonochemical synthesis of 4-(1H-indol-3-yl)thieno[2,3-*d*]pyrimidine derivatives **56** *via* a heteroarylation reaction in the presence of AcOH.



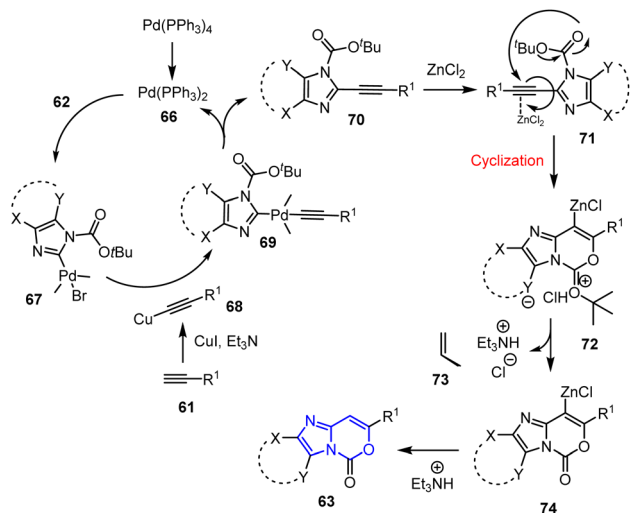
Scheme 15 Sonochemical synthesis of oxazinone derivatives **63** and **65**.

reaction times, and the use of an eco-friendly energy source (Scheme 15).

Following *in vitro* screening, compounds **65a**, **65b**, and **65c** were identified as preliminary leads for TNF- $\alpha$  inhibition. Furthermore, *in silico* docking studies using the TNF- $\alpha$  protein (PDB 7JRA and  $6 \times 81$ ) predicted **65a**, **63a**, **63b**, and **63c** as potential leads. These compounds interacted with common residues, such as LEU233, TYR135, TYR227, LEU133, ILE231, and LEU196 in 7JRA and TYR59, LEU57, TYR119, and GLY121 in  $6 \times 81$ . *In vitro* evaluations confirmed that **63a**, **63b**, and **63c** were the most active compounds. Additionally, structural analysis revealed that compounds bearing the tricyclic fused ring system 1H-benzo[4,5]imidazo[1,2-*c*][1,3]oxazin-1-one exhibited superior TNF- $\alpha$  inhibition capabilities than those containing a bicyclic fused ring (5H-imidazo[1,2-*c*][1,3]oxazin-5-one). SAR analysis indicated that the C-3 aryl group in the benzoimidazo-1,3-oxazinones followed the activity order:  $\text{C}_6\text{H}_5 > p\text{-MeC}_6\text{H}_4 > 2\text{-pyridyl} > p\text{-MeOC}_6\text{H}_4 > p\text{-ClC}_6\text{H}_4$ , whereas substitution with a 3-thienyl group at the C-3 position led to a reduced efficacy.

The reaction mechanism for the formation of products **63** begins with the ultrasound-assisted generation of the active Pd(0) species **66**, which undergoes oxidative addition to the halide **62**, forming the Pd(II) species **67**. Transmetalation with *in situ* generated Cu-acetylide **68** affords the heteroarene-Pd(II)-alkynyl complex **69**. Sonochemical conditions facilitate the subsequent reductive elimination to yield internal alkyne **70**, thereby regenerating the active Pd catalyst. Furthermore, activation of the **70** triple bond by  $\text{ZnCl}_2$  generates **71**, which



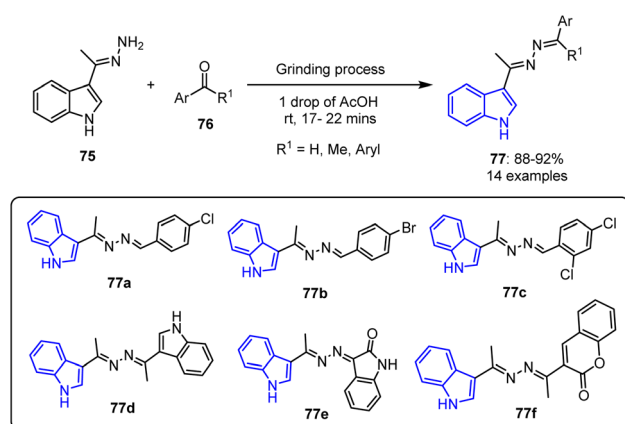


Scheme 16 Sonochemical coupling-cyclization mechanism for the synthesis of imidazo-1,3-oxazinones **63**.

undergoes *6-endo-dig* cyclization through intramolecular nucleophilic attack by the neighboring  $-\text{CO}_2^t\text{Bu}$  oxygen atom on the polarized triple bond, generating the cyclic organo-Zn intermediate **72**. The ultrasound-assisted release of 2-methylprop-1-ene **73** yields the neutral Zn-species **74**, which spontaneously quenches to form the final product **63** (Scheme 16).

## 2.3 Mechanochemical synthesis of anticancer agents

**2.3.1 Indole.** Ibrahim *et al.* reported an environmentally friendly synthesis of novel benzaldazine and ketazine derivatives **77**.<sup>83</sup> This method involved a solvent-free grinding technique using a catalytic amount of acetic acid to facilitate the condensation of various aldehydes and ketones **76** with 3-(1-hydrazineylideneethyl)-1*H*-indole **75** (Scheme 17). The anticancer potentials of the prepared compounds were evaluated against colon (HCT-116), liver (HepG2), and breast (MCF-7) cell lines using the MTT assay, using doxorubicin as the standard

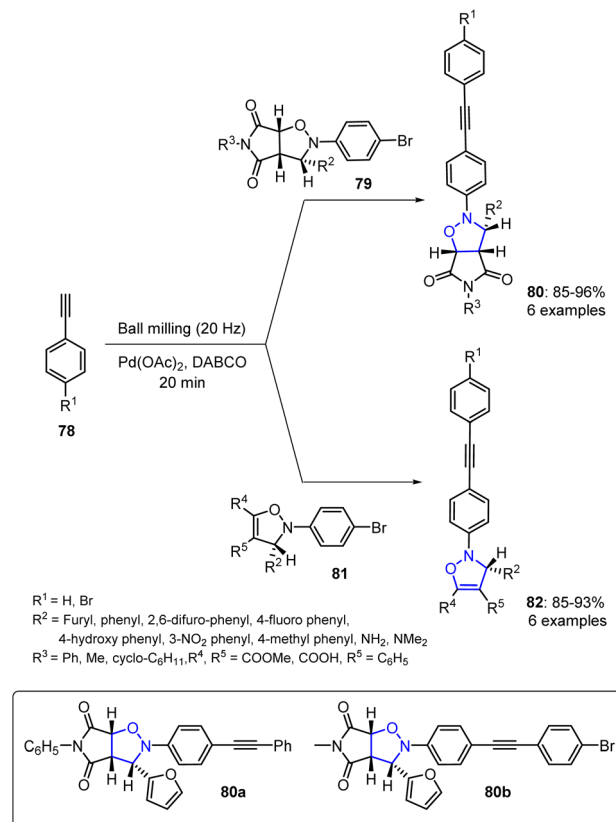


Scheme 17 Synthesis of benzaldazine and ketazine derivatives **63** using a grinding methodology.

reference drug. With  $\text{IC}_{50}$  values ranging from 4.27 to 8.15  $\mu\text{M}$ , a number of derivatives (*i.e.*, **77a**, **77b**, **77c**, **77d**, and **77e**) showed significant efficacies against HCT-116 cells, giving comparable or superior results to doxorubicin ( $\text{IC}_{50} = 5.23 \mu\text{M}$ ). With respect to the HePG-2 cell line, doxorubicin exhibited an  $\text{IC}_{50}$  value of 4.50  $\mu\text{M}$ , while compounds **77a**, **77b**, **77c**, **77d**, **77e**, and **77f** gave  $\text{IC}_{50}$  values ranging from 4.09 to 9.05  $\mu\text{M}$ . For the MCF-7 cell line, derivatives **77c**, **77d**, and **77e** demonstrated notable activities ( $\text{IC}_{50} = 6.19\text{--}8.39 \mu\text{M}$ ), in contrast to doxorubicin ( $\text{IC}_{50} = 4.17 \mu\text{M}$ ).

**2.3.2 Isoxazole.** Bhaskar and Esmita described the synthesis of novel heterocyclic derivatives **80** and **82** *via* a Sonogashira cross-coupling protocol and a mechanochemical strategy.<sup>84</sup> This reaction was conducted in a ball mill under solvent-free conditions, emphasizing the efficient and environmentally sustainable nature of their method. The ball-milling process enabled effective coupling by providing the necessary mechanical energy to activate the reactants, eliminating the requirement for conventional heating or toxic solvents (Scheme 18).

Screening of the synthesized compounds indicated that the majority displayed notable cytotoxic effects against prostate, leukemia, breast, and lung cancer cell lines. Among the cyclo-adducts, isoxazolidine derivatives **80a** and **80b** exhibited optimal  $\text{IC}_{50}$  values against the HCT-8, PC-3, and MDA-MB-23 cell lines, demonstrating superior activities than other



Scheme 18 Sonogashira cross-coupling reaction to generate isoxazoline **82** and isoxazolidine **80**.

isoxazolidine and isoxazoline analogues. Based on these results, derivatives **80a** and **80b** were selected for further cell cycle analysis, which is currently underway.

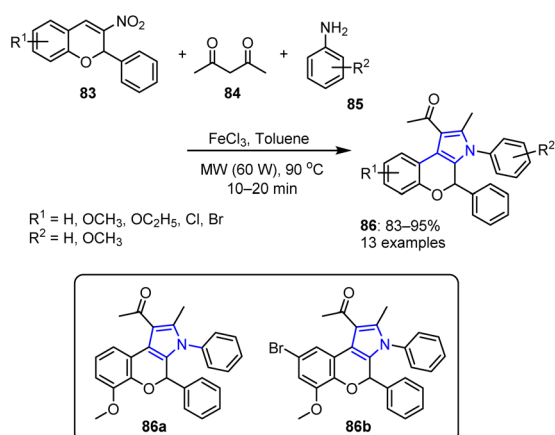
### 3. N-heterocycles with antibacterial activities

Antibacterial active compounds are substances that inhibit bacterial growth or kill bacteria by targeting essential cellular processes. They function *via* various mechanisms, including cell wall disruption, the inhibition of protein synthesis, interfering with DNA replication, and blocking metabolic pathways.<sup>85,86</sup>

#### 3.1 Microwave-assisted synthesis of antibacterial agents

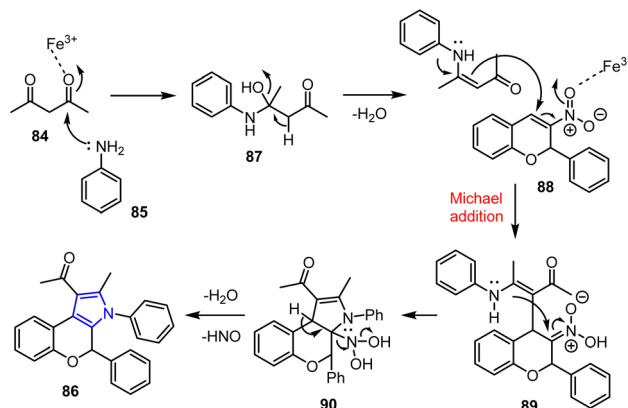
**3.1.1 Pyrrole.** Baral *et al.* reported the synthesis of novel fused chromene-pyrrole derivatives **86**.<sup>87</sup> In this process, numerous functionalized *2H*-chromenes **83** were reacted with acetylacetone **84** and aniline **85** in the presence of FeCl<sub>3</sub> as a catalyst in toluene under 60 W MW irradiation for 15 min. As detailed in Scheme 19, the desired chromene-fused pyrrole derivatives **86** were obtained in good yields.

As a Lewis acid, FeCl<sub>3</sub> catalyzes the multicomponent reaction by activating the carbonyl oxygen atom of the 1,3-dicarbonyl compound. The first step involves the nucleophilic addition of acetylacetone **84** to aniline **85** to generate  $\beta$ -enaminocarbonyl intermediate **87**. Subsequently, intermediate **89** is produced *via* a Michael addition reaction with 3-nitro-*2H*-chromene **88**, which is catalyzed by FeCl<sub>3</sub>. Compound **89** then undergoes an intramolecular cyclization reaction, resulting in the formation of an intermediate dihydropyrrole **90**, which eventually eliminates HNO and water to generate the desired product **86**, which possesses a fused heterocyclic structure (Scheme 20).



Method	Solvent	Reaction time	Yield
Conventional heating (80 °C)	Toluene	15 h	-
MW	Toluene	15 min	90%

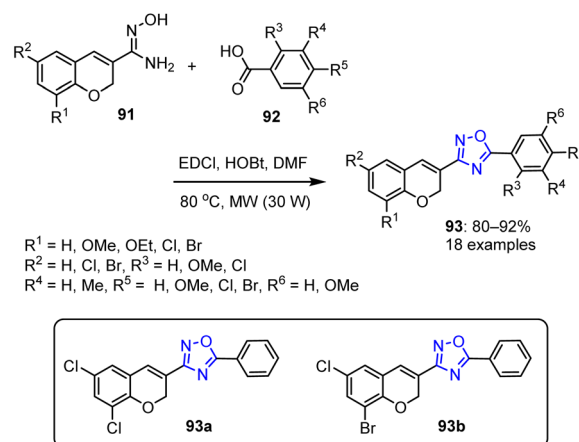
Scheme 19 Synthesis of chromene-fused pyrrole derivatives **86** from 3-nitro-*2H*-chromenes **83**.



Scheme 20 Plausible mechanism for the MW-assisted one-pot synthetic protocol for the preparation of *2H*-chromene-fused pyrrole derivative **86**.

The produced compounds were evaluated using the agar-well diffusion technique, with gentamicin acting as the reference antimicrobial agent. The assays focused on the Gram-positive bacterium *Staphylococcus aureus* (MTCC7443) and the Gram-negative bacterium *Escherichia coli* (MTCC614), enabling the assessment of the minimum inhibitory concentration (MIC) and the inhibition zone. Among the synthesized compounds, **86a** and **86b** showed significant activities against *E. coli* and *S. aureus*. Compound **86b** exhibited the greatest activity, producing inhibition zones of 18 and 99 mm against *E. coli* and *S. aureus*, respectively, at an MIC of 20  $\mu\text{g mL}^{-1}$ . This level of activity is almost comparable to that of gentamicin, which shows inhibition zones of 17 and 19 mm against *E. coli* and *S. aureus*, with an MIC of 20  $\mu\text{g mL}^{-1}$ .

**3.1.2 Oxadiazole.** The same research group synthesized chromene-fused oxadiazole derivatives **93** with yields ranging from 80% to 92%.<sup>88</sup> This involved the reaction of *2H*-chromene-3-carboximidamide **91** with various carboxylic acid derivatives **92** in anhydrous DMF. The reaction was facilitated by EDCI/



Scheme 21 Microwaved-assisted synthetic route for the preparation of fused chromene-oxadiazole derivatives **93**.

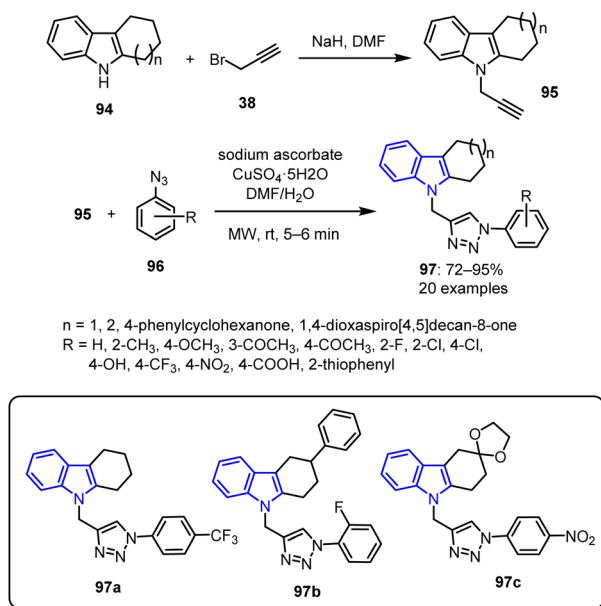


HOBt as the coupling agent and was conducted under MW irradiation (Scheme 21).

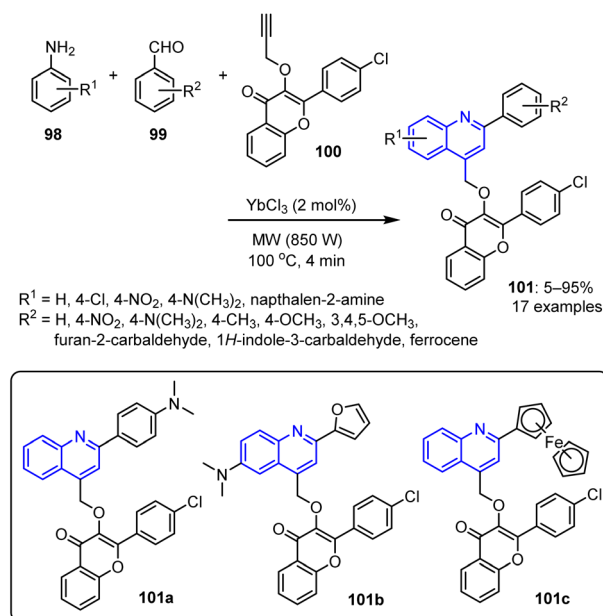
Among the produced compounds, **93a** and **93b** were recognized as the most effective antibacterial agents. These compounds exhibited robust activities against *E. coli* (MTCC614) and *Klebsiella pneumoniae* (MTCC4031). Furthermore, they specifically bound to the DNA gyrase of the targeted bacteria.

**3.1.3 Indole.** Ashok *et al.* outlined a synthetic pathway for the synthesis of functionalized 1,2,3-triazole-based carbazole derivatives **97** bearing indole and triazole as substituents.<sup>89</sup> Initially, diverse tetrahydrocarbazoles **94** were synthesized by reacting substituted cyclohexanones with phenyl hydrazine.<sup>90</sup> The resulting tetrahydrocarbazoles **94** then underwent a base-catalysed *N*-alkylation with propargyl bromide **38** in DMF, leading to the formation of *N*-propynyl tetrahydrocarbazoles **95**. These alkynes were subsequently reacted with various aromatic azides **96** via a copper-catalyzed Huisgen [3 + 2] cycloaddition reaction under MW irradiation in the presence of sodium ascorbate and CuSO<sub>4</sub>. This process yielded functionalized derivatives **97** in good yields ranging from 72% to 95% (Scheme 22).

All synthesized compounds were evaluated using well diffusion techniques at concentrations of 10 and 20 μM. Ampicillin served as the reference antibiotic and the inhibition zones were measured in millimeters (mm) and compared with those of the standard drug nystatin. The assays were performed against three Gram-negative bacterial strains as well as two Gram-positive strains. Among the synthesized compounds, those bearing *p*-(trifluoromethyl)phenyl **97a**, *o*-fluorophenyl **97b**, and *p*-nitrophenyl **97c** substituents demonstrated excellent antibacterial efficacies against all tested strains.



Scheme 22 Synthetic pathway for the preparation of novel indole-substituted functionalized 1,2,3-triazole-based carbazole derivatives **97**.



Scheme 23 Synthesis of quinolin-4-yl-methoxychromen-4-ones **101**.

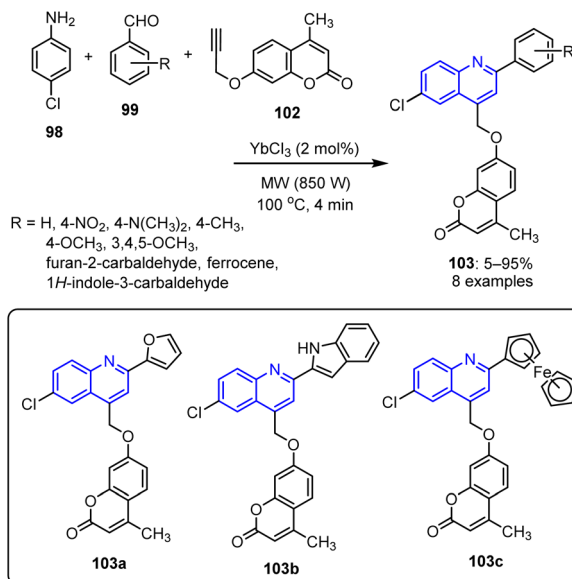
**3.1.4 Quinoline.** Sumit *et al.* reported the synthesis of quinolin-4-ylmethoxychromen-4-ones **101**.<sup>91</sup> The reaction sequence involved the coupling of aryl-substituted propynyloxy chromenone **100** with various substituted anilines **98**, followed by the addition of substituted aromatic aldehydes **99**, under MW-assisted conditions. The process afforded the target compounds **101** with yields varying from 5% to 95% (Scheme 23).

Among the synthesized compounds, those featuring an electron-donating group (*e.g.*, dimethyl amine, **101a**) and compounds containing heterocyclic structures (*e.g.*, furan, **101b** and ferrocene, **101c**) displayed significant antibacterial activities. Specifically, these compounds demonstrated remarkable-to-adequate MICs (0.39–1.56 mg mL<sup>-1</sup>) against *S. aureus*, *E. coli*, and *B. subtilis*.

The same group further synthesized aryloxy chromen-2-ones **103** using a similar synthetic protocol.<sup>91</sup> This involved the reaction of propynyloxy-2*H*-chromen-2-one **102** with 4-chloro aniline **98** and various substituted aromatic aldehydes **99**. This procedure, which was conducted in the presence of YbCl<sub>3</sub> under MW exposure at 100 °C for 4 min, produced the corresponding quinolin-4-yl methoxy-chromen-2-one derivatives **103** in good yields of up to 94% (Scheme 24). Similar to the quinolin-4-ylmethoxychromen-4-ones **101**, the synthesized quinolin-4-yl methoxy-chromen-2-ones bearing heterocyclic substituents (*i.e.*, **103a**, **103b**, and **103c**) exhibited outstanding-to-satisfactory MICs against *S. aureus*, *E. coli*, and *B. subtilis*.

This one-pot reaction follows a domino pathway, namely imine formation, addition, cyclization, and oxidation pathways, which were catalysed by YbCl<sub>3</sub>. Yb<sup>3+</sup>, which is a hard Lewis acid, coordinates with the imine nitrogen of **104**, enhancing its electrophilicity and promoting nucleophilic attack. Its small ionic radius and water tolerance boost its efficiency, facilitating

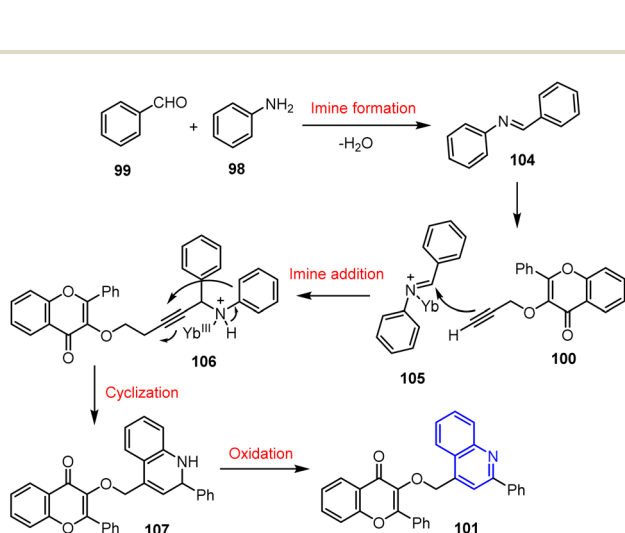




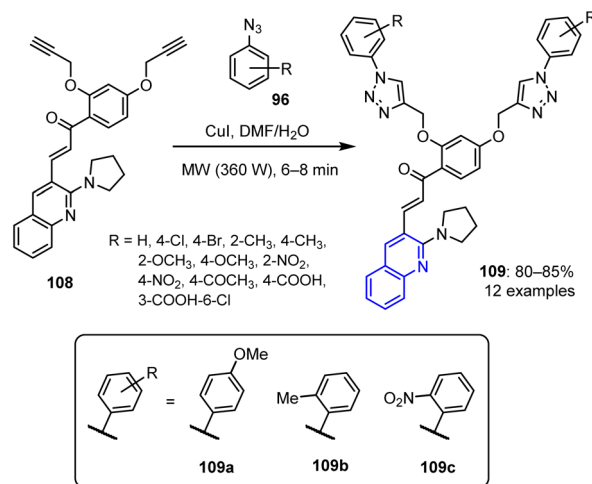
Scheme 24 YbCl<sub>3</sub>-catalyzed synthetic protocol for the preparation of arylmethoxy-chromen-2-one derivatives **103**.

cyclization and oxidation to give a high selectivity and yield (Scheme 25).

Pradeep *et al.* reported the synthesis of triazole-based derivatives *via* a [3 + 2] cycloaddition reaction.<sup>92</sup> This involved the reaction of 2,4-dipropynyloxy- $\alpha$ -substituted acetophenone **108** with aryl azides **96** under MW irradiation at 360 W (Scheme 26). The resulting products, namely pyrrolidinyl-quinoline chalcone hybrid bis-1,2,3-triazoles **109**, were obtained in yields of up to 84% after only 6–8 min of irradiation. The starting material, dipropynyloxy- $\alpha$ -substituted acetophenone **108**, was also synthesized using MW irradiation. Specifically, this was performed by reacting a methanolic solution of 2-pyrrolidinyl-3-quinoline carbaldehyde and 1-(2,4-bis(prop-2-yn-1-yloxy)phenyl)ethanone in the presence of KOH.<sup>92</sup>



Scheme 25 Proposed reaction mechanism for the YbCl<sub>3</sub>-catalyzed one-pot synthesis of quinolin-4-yl methoxy-chromen-4-ones **101**.

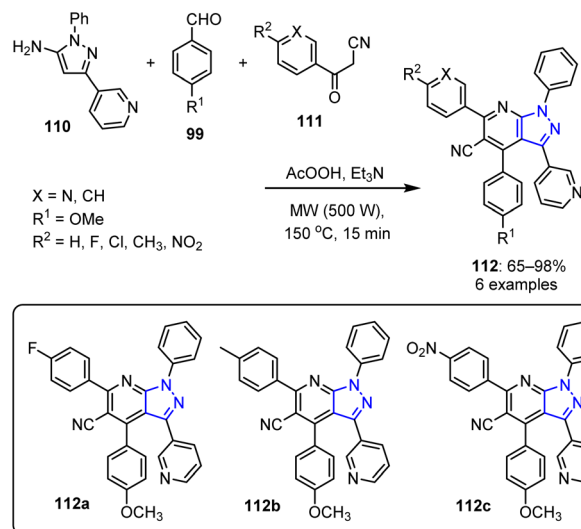


Scheme 26 Synthesis of pyrrolidinyl-quinoline- and 1,2,3-triazole-based chalcone derivatives **109**.

Among the synthesized compounds, the compounds bearing 4-methoxyphenyl **109a**, 2-methylphenyl **109b**, and 2-nitrophenyl **109c** substitutions exhibited strong antibacterial activities. Specifically, they were effective against four bacterial strains, namely *Enterococcus faecalis*, *K. pneumoniae*, *S. aureus*, and *E. coli*. Ampicillin was employed as the reference standard.

**3.1.5 Pyrazole.** El-Borai *et al.* reported a novel one-pot, multicomponent approach for the synthesis of pyrazolo[3,4-*b*]pyridine derivatives **112** under MW-assisted conditions.<sup>93</sup> In an acetic acid medium, 5-amino-1-aryl pyrazolopyridine **110** was reacted with 4-anisaldehyde **99** in the presence of triethylamine. The reaction was performed at 150 °C for 15 min, affording the desired pyrazolo[3,4-*b*]pyridine derivatives **110** in yields of up to 98% (Scheme 27).

The newly synthesized 1-aza indazole derivatives **112a** and **112b** exhibited moderate antibacterial activities against both



Scheme 27 MW-assisted synthesis of 1-aza indazole derivatives **112**.

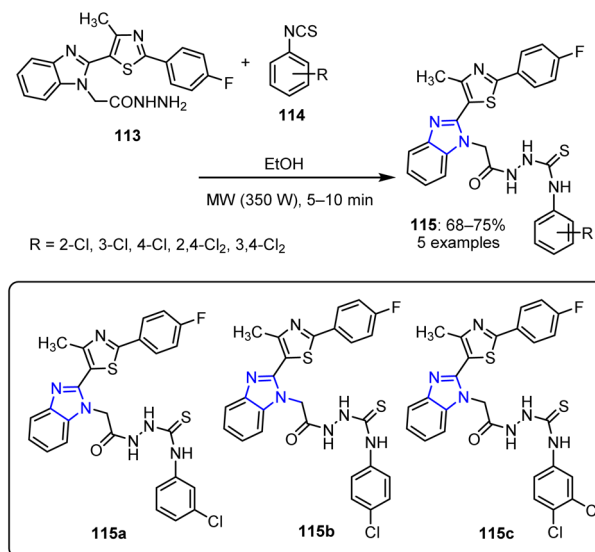


Gram-negative bacteria (*Enterobacter cloacae*, *E. coli*, and *Serratia*) and Gram-positive bacteria. Additionally, compound **112c** exhibited antifungal properties against *Fusarium oxysporum* and *Penicillium expansum*.

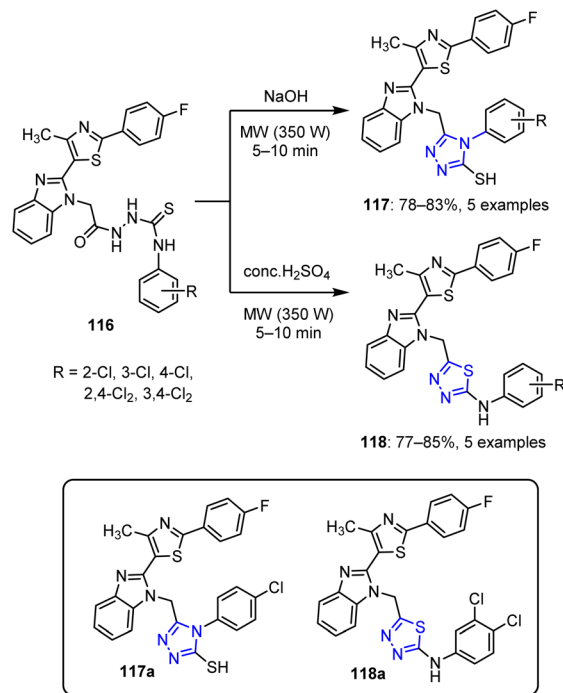
**3.1.6 Imidazole.** Due to its electron-rich nature and ability to participate in hydrogen bonding and metal coordination, imidazole serves as a crucial scaffold in pharmaceuticals, catalysis, and bioinorganic chemistry. The C-2 and C-4/C-5 positions are particularly reactive, enabling diverse functionalization for advanced synthetic applications. In this context, Darekar *et al.* reported a novel synthetic method for creating thiosemicarbazide-based imidazole derivatives **115**, as shown in (Scheme 28).<sup>94</sup> Specifically, they synthesized acetohydrazide-substituted heterocycles **113** through a series of reactions. These compounds were subsequently treated with aryl isothiocyanates **114** under MW irradiation at 350 W for 5–10 min, resulting in the formation of thiosemicarbazide-based imidazole derivatives **115**.

The compounds bearing substituents at the *meta* and *para* positions (**115a**, **115b**, and **115c**) exhibited significant activities toward Gram-positive and Gram-negative bacterial strains. The bacterial strains selected for evaluation included *Bacillus subtilis* (NCIM 2063), *E. coli* (NCIM 2810), *S. aureus* (NCIM 2079), and *Salmonella abony* (NCIM 2257).

**3.1.7 Triazoles and thiadiazoles.** The same authors expanded their research by synthesizing 1,2,4-triazole derivatives **117** and 1,3,4-thiadiazoles **118** from thiosemicarbazide-cored imidazole derivatives **116** (Scheme 29).<sup>94</sup> When compound **116** was treated with a base under MW irradiation at 350 W for 5–10 min, 1,2,4-triazole derivatives **117** were formed. On the other hand, treating compound **116** with acid under MW conditions yielded 1,3,4-thiadiazoles **118**. In the 1,2,4-triazole series, *para*-substituted derivative **117a** exhibited a superior activity, while in the 1,3,4-thiadiazole series, both *para* and *meta* substitutions (*e.g.*, compound **118a**) led to enhanced activities.



Scheme 28 Synthesis of thiosemicarbazide-based imidazole derivatives **115**.



Scheme 29 Synthesis of 1,2,4-triazole derivatives **117** and 1,3,4-thiadiazoles **118** from compound **116**.

## 4. N-heterocycles with antifungal activities

Antifungal N-heterocycles are nitrogen-containing heterocyclic compounds that inhibit fungal growth by targeting key cellular processes. They act by disrupting cell membranes, inhibiting ergosterol biosynthesis, interfering with DNA/RNA synthesis, or blocking essential fungal enzymes. Their structural diversities and hydrogen bonding abilities enhance their binding to fungal targets, rendering them valuable in the field of antifungal drug development.<sup>95,96</sup>

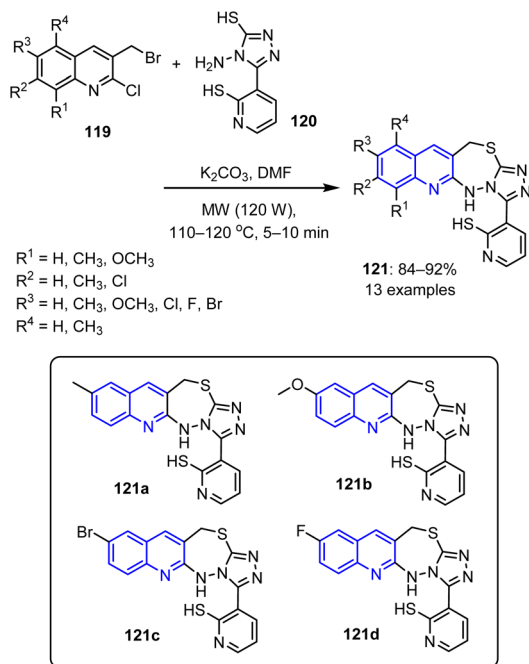
### 4.1 Microwave-assisted synthesis of anti-fungal compounds

**4.1.1 Quinolines.** Kausar *et al.* reported the reaction of the substituted 4-amino-1,2,4-triazole-3-thiol **120** with 3-(bromomethyl)-2-chloro-quinoline derivatives **119** in DMF.<sup>97</sup> Subsequent treatment of the reaction mixture with potassium carbonate under MW irradiation at 120 W for 5–10 min led to the formation of triazolothiadiazepinyl quinolines **121** (Scheme 30).

The antiviral properties of the synthesized molecules were subsequently evaluated, revealing that compounds bearing methyl **121a**, methoxy **121b**, bromo **121c**, and fluoro **121d** substituents exhibited MIC values. These compounds exhibited significant inhibitory effects against *Aspergillus fumigatus*, indicating their promising antiviral potential.

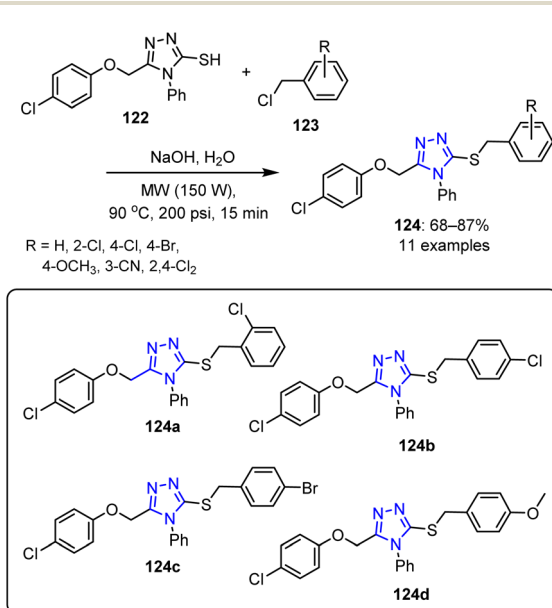
**4.1.2 Triazole.** Min *et al.* reported the synthesis of novel 1,2,4-triazole-based thioethers **124**.<sup>98</sup> This approach was based on the reaction of substituted 1,2,4-triazole-3-thiol **122** with substituted benzyl chloride **123** in DMF, employing NaOH as



Scheme 30 Synthesis of triazolothiadiazepinyl quinolines **121**.

the base. The reaction was conducted under optimized conditions using a CEM Discover Focused Synthesizer, affording the desired thioether derivatives in yields ranging from 68% to 87% (Scheme 31).

Among the synthesized novel 1,2,4-triazole-cored thioether derivatives, the compounds bearing 2-chlorobenzene **124a**, 4-chlorobenzene **124b**, 4-bromobenzene **124c**, and 4-methoxybenzene **124d** moieties exhibited strong inhibition against the fungus *Corynespora cassicola*. Additionally, some of these

Scheme 31 Synthetic procedure for the preparation of novel 1,2,4-triazole-based thioethers **124**.

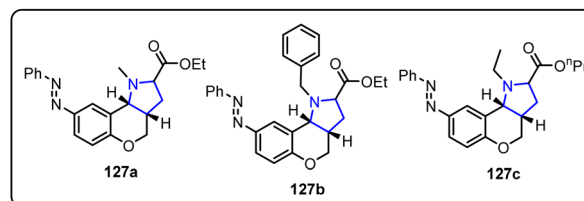
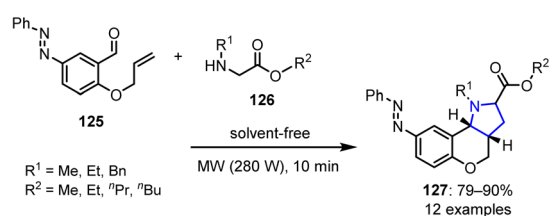
compounds also demonstrated promising antiviral activities against *Pythium ultimum* Trow.

**4.1.3 Pyrrolidine.** The intramolecular azomethine ylide cycloaddition of *O*-allyl-5-phenyldiazenylsalicylaldehyde **125** with various esters **126** under MW irradiation produced aryl-diazenylchromeno[4,3-*b*]pyrrolidines **127** in yields of 80–90% (Scheme 32).<sup>99</sup> While some of the synthesized compounds exhibited antibacterial and antitubercular activities, compounds **127a–127c** showed exceptional antifungal activities against *Candida albicans*, with MIC values lower than that of the standard drug griseofulvin. Additionally, all synthesized compounds demonstrated moderate-to-strong activities against various bacterial cell lines.

**4.1.4 Pyridine.** Acosta *et al.* reported the synthesis of a novel series of pyrazolo naphthyridin-5-amines **130** using a MW-assisted reaction.<sup>100</sup> This involved the  $\text{ZnCl}_2$ -catalyzed reaction of heterocyclic aminonitriles **128** and cyclic carbonyl compound **129**, producing the desired compounds in yields ranging from 55% to 80% (Scheme 33).

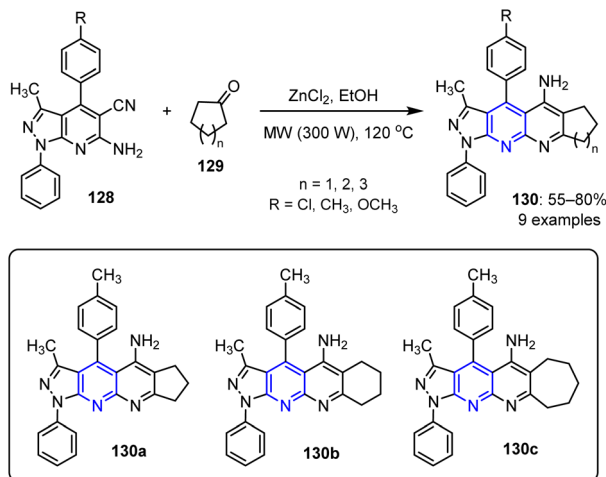
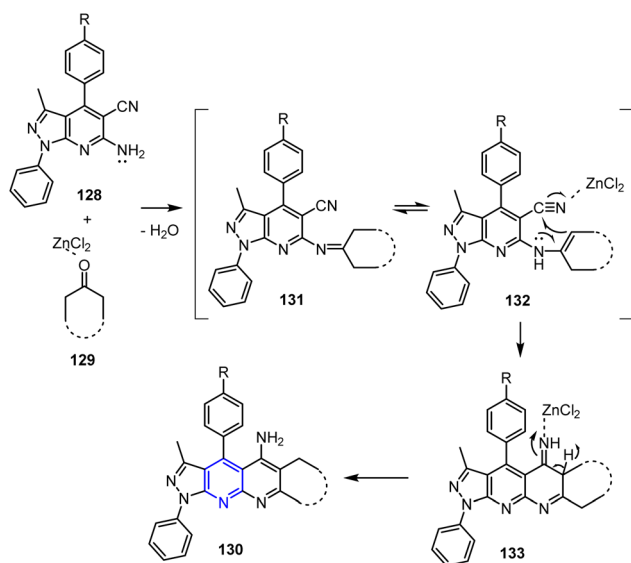
The hypothesized mechanism underlying the cyclization reaction between compounds **128** and **129** involves initial imine formation (intermediate **131**) through a typical Friedländer reaction.<sup>101,102</sup> This intermediate then undergoes an intramolecular nucleophilic attack at the nitrile group, resulting in ring closure and formation of the final product **130**. This sequence highlights the efficiency of the Friedländer approach in constructing nitrogen-containing heterocycles (Scheme 34).

In 2006, Chhillar *et al.* synthesized novel dialkyl-4-aryl-2,6-dimethyl-1,4-dihydropyridin-3,5-dicarboxylates **137** using the Biginelli cyclocondensation method.<sup>103</sup> This reaction utilized ethyl/methyl acetoacetate **136**, urea **135**, and an aromatic aldehyde **134**, and was performed under MW irradiation at 850 W



Method	Compound	Solvent	Duration	Yield
Conventional heating (81–190°C)	<b>127a-c</b>	Toluene	6.5–8 h	62–71%
MW	<b>127a-c</b>	Solvent-free	10 min	83–87%

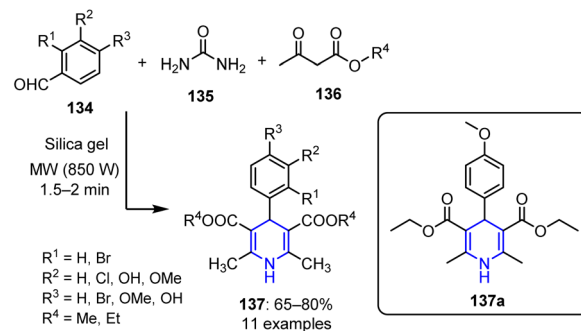
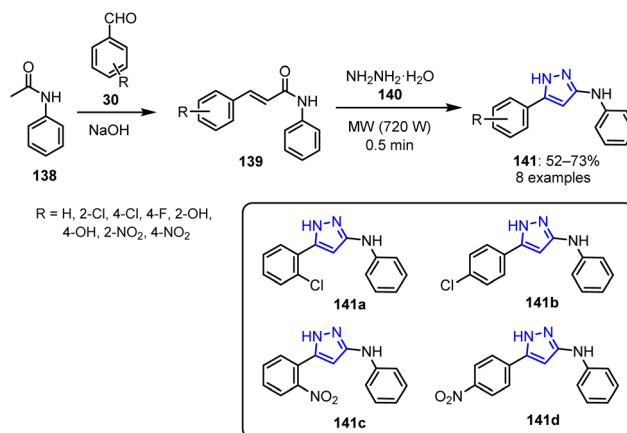
Scheme 32 Synthesis of phenyldiazenylchromeno fused pyrrolidines **127**.

Scheme 33 Synthesis of naphthyridine derivatives **130**.Scheme 34 Plausible mechanism for the synthesis of pyrazolo naphthyridin-5-amines **130**.

for up to 2 min. The desired products were obtained in moderate yields (Scheme 35).

The antifungal activities of all synthesized compounds were subsequently evaluated using the disc diffusion assay, micro-broth dilution assay, and percentage spore germination inhibition assay against *A. fumigatus* and *C. albicans*. While all compounds demonstrated notable efficacies, diethyl 4-(4-methoxyphenyl)-2,6-dimethyl-1,4-dihydropyridine-3,5-dicarboxylate **137a** exhibited the strongest antifungal activity. Additionally, the colony-forming unit assay confirmed that compound **137a** possesses a strong anti-*Candida* action and effectively inhibits the growth of *A. fumigatus*. This suggests that the 4-methoxyphenyl group plays a crucial role in the ability of dihydropyridine to suppress *A. fumigatus* development.

**4.1.5 Pyrazole.** A methanolic solution of benzaldehydes **30** and acetanilide **138** was irradiated at 540 W in the presence of

Scheme 35 Synthesis of dialkyl-4-aryl-2,6-dimethyl-1,4-dihydropyridin-3,5-dicarboxylates **137**.Scheme 36 Synthetic route to bioactive pyrazolines **141**.

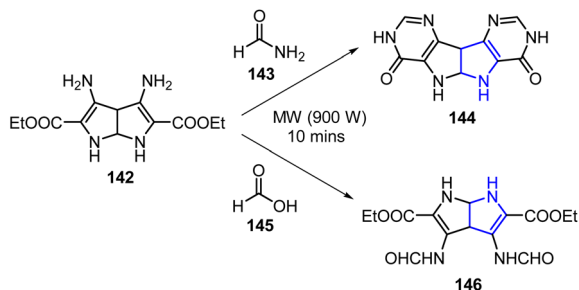
aqueous  $\text{NaOH}$  to produce various acrylamides **139**.<sup>104</sup> The acrylamides were subsequently treated with hydrazine hydrate **140** in the presence of glacial acetic acid under MW irradiation at  $720\text{ W}$ , resulting in the formation of the corresponding pyrazolines **141** with good yields ranging from 52% to 73% (Scheme 36).

The antifungal activities of all synthesized pyrazolines were evaluated using the poisoned food technique, with Bavistin as the standard drug. The compounds bearing chloro substituents at the *ortho* **141a** and *para* **141b** positions exhibited  $\text{ED}_{50}$  values of  $930$  and  $760\ \mu\text{g mL}^{-1}$  against *D. maydis*, respectively. These compounds showed inhibition comparable to Bavistin at  $1000\ \mu\text{g mL}^{-1}$  against *R. solani*. Compounds with nitro groups **141c** and **141d** also demonstrated similar inhibition activities at all concentrations.

## 5. N-heterocycles with antimicrobial activities

N-heterocyclic compounds exhibit remarkable antimicrobial properties by targeting key pathways that are essential for microbial survival and growth. Their effectiveness against a broad spectrum of microbial pathogens is attributed to their





Scheme 37 MW-assisted synthesis of novel pyrrolo[2,3-*b*]pyrrole derivatives **144** and **146**.

ability to disrupt essential biological processes, including cell wall synthesis, protein formation, and DNA replication.<sup>105–107</sup>

## 5.1 Microwave-assisted synthesis of antimicrobial agents

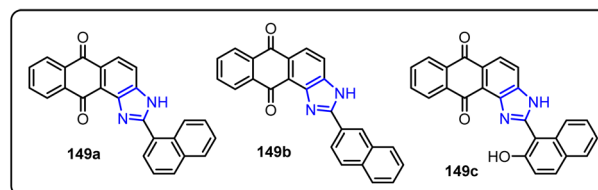
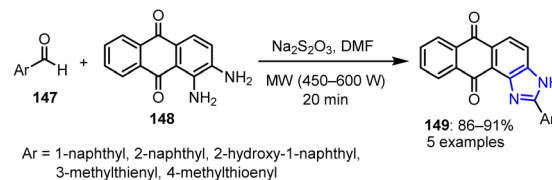
**5.1.1 Pyrrole.** Moumen *et al.* developed a MW-assisted synthesis of novel pyrrolo[2,3-*b*]pyrrole derivatives **144** and **146** using formamide **143** and formic acid **145** as substituents, affording the desired compounds in appreciable yields (Scheme 37).<sup>108</sup> The synthesized compounds were subsequently evaluated for their biological activities. Several derivatives exhibited moderate-to-good antimicrobial activities. For example, compound **144** showed a moderate efficacy against *Pseudomonas aeruginosa* (MIC: 50  $\mu\text{g mL}^{-1}$ ), although it was less potent than ciprofloxacin (MIC: 25  $\mu\text{g mL}^{-1}$ ). Additionally, compound **146** exhibited a significant activity against *S. aureus*, showing effectiveness comparable to that of ciprofloxacin, though it was approximately half as potent as ampicillin. Meanwhile, compound **144** demonstrated an antifungal activity against *C. albicans* that reached approximately 25% that exhibited by clotrimazole, while also demonstrating the highest antioxidant capacity with a 59% radical scavenging activity. Additionally, the majority of the synthesized derivatives displayed encouraging anticancer activities across the three evaluated cell lines.

## 6. N-heterocycles with anti-inflammatory activities

N-heterocyclic compounds are key scaffolds in anti-inflammatory drug development since their nitrogen atoms promote interactions with biological targets, such as COX-2 and the cytokine receptors. Additionally, their structural versatility allows for strong binding, good bioavailabilities, and superior metabolic stabilities, often resulting in improved efficacies and reduced toxicities compared with those of non-heterocyclic compounds.<sup>109,110</sup>

### 6.1 Microwave-assisted synthesis of anti-inflammatory agents

**6.1.1 Imidazole.** Sondhi *et al.* reported a series of imidazole derivatives with promising potential for exhibiting enhanced anti-inflammatory and anticancer activities. The cyclization of



Compound	Reaction time		Yield	
	Conventional heating(130°C)	MW	Conventional heating(130°C)	MW
<b>149a</b>	10 h	20 min	89%	90%
<b>149b</b>	12 h	20 min	89%	91%
<b>149c</b>	12 h	20 min	88%	88%

Scheme 38 Synthesis of 3-aryl-anthra[1,2-*d*]imidazole-6,11-diones **149**.

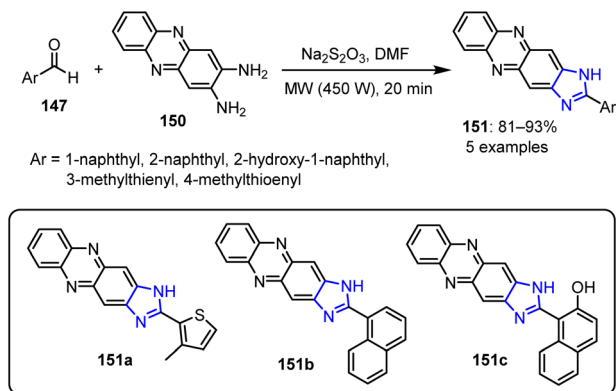
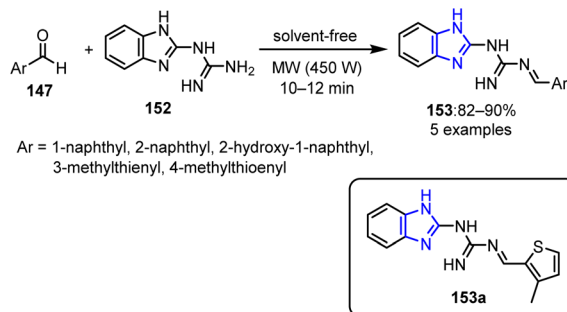
aromatic aldehydes **147** with 1,2-diaminoanthraquinone **148** was carried out under MW irradiation at 450 W for 5 min.<sup>111</sup> Using sodium metabisulfite and DMF as catalysts, this reaction yielded the corresponding 3-aryl-anthra[1,2-*d*]imidazole-6,11-diones **149** (Scheme 38).

All synthesized compounds were evaluated for their anti-inflammatory and anticancer activities using the carrageenan-induced paw edema model. Ibuprofen, which was used as the reference drug, displayed the highest anti-inflammatory effect at approximately 39% inhibition with an oral dose of 50 mg  $\text{kg}^{-1}$ . Among the tested compounds, the compound bearing a 2-naphthalenyl substituent (**149b**) exhibited an anti-inflammatory activity that was nearly equivalent to that of ibuprofen. In contrast, 1-naphthalenyl-substituted derivatives **149a** and **149c** exhibited enhanced anticancer activities.

Another series of imidazole derivatives **151** was synthesized under the same conditions, using phenazine-2,3-diamine **150** instead of 1,2-diaminoanthraquinone **148** as the starting material (Scheme 39). Similar to the previous series, naphthalenyl-substituted derivatives **151b** and **151c** demonstrated anticancer activities, while compound **151a** exhibited a 38% anti-inflammatory activity when administered orally at a dose of 50 mg  $\text{kg}^{-1}$ .

The authors further extended their research by synthesizing imidazole-cored guanidine derivatives **153**.<sup>111</sup> This synthetic approach employed 2-guanidinobenzimidazole **152** and aromatic aldehyde **147** as starting reagents. The reactions were conducted without the use of solvent, utilizing MW irradiation at 450 W for 10–20 min to yield the target products with yields up to 90% (Scheme 40). The imidazole-based guanidine structure bearing a thiophene derivative **153a** exhibited promising anti-inflammatory properties comparable to those of ibuprofen.



Scheme 39 Synthesis of 1-aryl-imidazo[4,5-*b*] phenazine 151.Scheme 40 Synthesis of 1-(1*H*-benzo[*d*]imidazol-2-yl)-3-((aryl)methylene)guanidines 153.

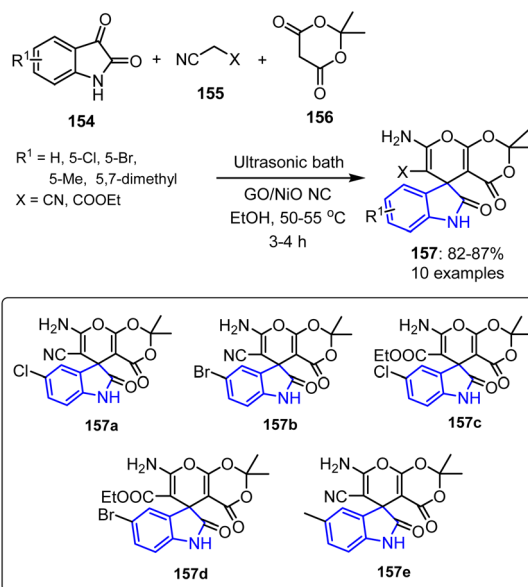
However, no other compounds in this series showed anticancer activity.

## 6.2 Sonochemical synthesis of anti-inflammatory agents

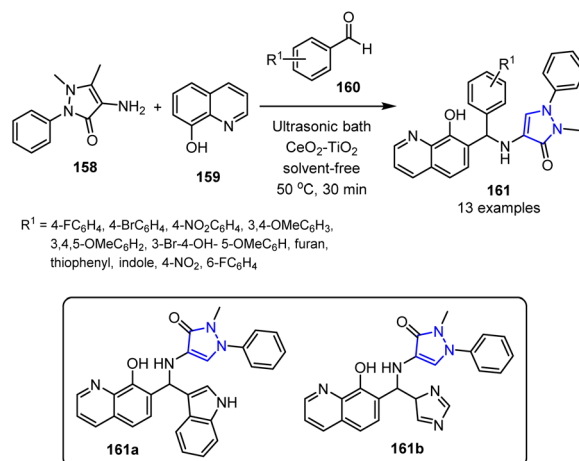
**6.2.1 Indole.** Khushboo *et al.* established an efficient synthetic approach for the preparation of spiroindole derivatives 157, achieving yields between 84% and 87% (Scheme 41). This method employed a catalytic quantity of a graphene oxide-supported nickel oxide nanocomposite (GO/NiO NC) as a highly active heterogeneous catalyst under ultrasonic irradiation. Remarkably, the GO/NiO NC catalyst exhibited a good recyclability, retaining its catalytic efficiency over three successive cycles with only a minor reduction in activity.<sup>112</sup>

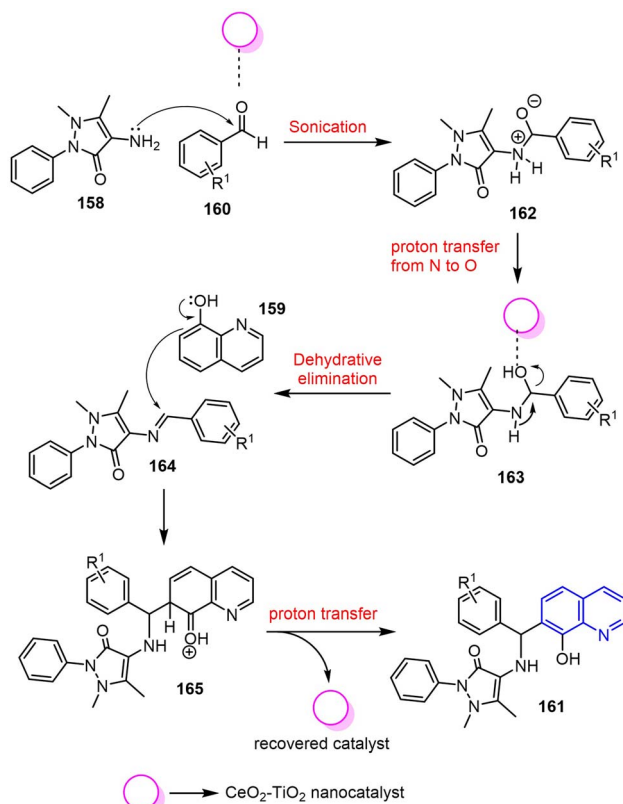
The synthesized spiroindole derivatives, particularly compounds 157a–157e, demonstrated significant anti-inflammatory activities by effectively preventing protein denaturation at all tested concentrations, indicating their potential for therapeutic use. Specifically, compound 157b exhibited the strongest anti-inflammatory effect, with inhibition rates ranging from 43.53% to 55.75% at concentrations of 20–100 mg L<sup>-1</sup>. This compound also displayed the lowest IC<sub>50</sub> value (55.85 mg L<sup>-1</sup>), rendering it the most potent compound in the series.

In another study, Bhaskar *et al.* developed an efficient, eco-friendly, and straightforward method for synthesizing bioactive antipyrene-linked quinoline analogues 161 using

Scheme 41 Synthesis of spiro[indoline-3,5'-pyrano[2,3-*d*]-[1'3']dioxine] derivatives 157.

a recyclable CeO<sub>2</sub>-TiO<sub>2</sub> nanocatalyst and ultrasonic irradiation.<sup>113</sup> This green approach leverages the synergistic effects of the nanocatalyst and ultrasound-assisted multicomponent reactions, enabling rapid hybrid construction with high yields under solvent-free conditions, thereby saving time, energy, and costs. The antibacterial and antioxidant activities of the synthesized compounds were subsequently assessed, with 161a and 161b demonstrating notable potencies in both cases (Scheme 42). Compared to conventional catalysts, the biogenically synthesized CeO<sub>2</sub>-TiO<sub>2</sub> nanocatalyst offers a superior performance, delivering higher yields in shorter reaction times, with an excellent reusability and minimal leaching. These findings underscore the potential of antipyrene hybrids for use

Scheme 42 CeO<sub>2</sub>-TiO<sub>2</sub>-catalyzed synthesis of antipyrene-linked quinolines 161.



Scheme 43 Plausible reaction mechanism for the  $\text{CeO}_2\text{-TiO}_2$  nanocatalyzed synthesis of quinoline analogues **161**.

as valuable frameworks in the development of novel pharmaceutical agents.

**6.2.2 Quinoline.** The synthesis of quinoline derivatives **161** involved a  $\text{CeO}_2\text{-TiO}_2$  nanocatalyst-mediated activation of aromatic aldehydes **160**, which increased the electrophilicity of the carbonyl carbon. This facilitated condensation with 4-aminoantipyrine **158**, followed by proton transfer and dehydration to form a Schiff base intermediate **163**.<sup>114,115</sup> Subsequently, this intermediate reacted with 8-hydroxyquinoline **159**, undergoing cyclization to yield the target compounds **161** (Scheme 43).

In this reaction, the nanocatalyst plays a dual role, initially activating the aldehyde, and later deprotonating the quinoline hydroxyl group, ultimately enhancing the nucleophilicity and accelerating Schiff base formation. This promotes a faster, solvent-free reaction with a high efficiency, and the nanocatalyst can be easily recovered and reused, thereby supporting the principles of green synthesis.

## 7. N-heterocycles with antitubercular activities

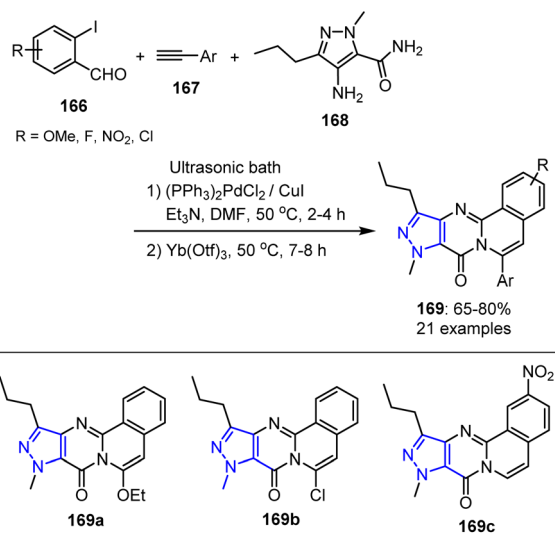
Nitrogen-containing ring-structured N-heterocyclic compounds have been demonstrated to exhibit potent anti-mycobacterial action. Specifically, scaffolds such as triazoles, pyridines, and quinolines interfere with various bacterial processes, including DNA replication and cell wall construction. Two important

examples of such compounds are bedaquiline and isoniazid. The potencies and structural adaptabilities of these substances render them essential for the development of TB drugs.<sup>116,117</sup>

### 7.1 Sonochemical synthesis of antitubercular agents

**7.1.1 Pyrazole.** Venkateswara *et al.* developed a synthetic protocol for a series of molecules containing the 4-amino-1-methyl-3-propyl-1H-pyrazole-5-carboxamide fragment **168** as potential chorismate mutase (CM) inhibitors.<sup>118</sup> This approach employed a Sonogashira coupling reaction between 2-iodobenzaldehydes **166** and a terminal alkyne **167**, generating 2-alkynylbenzaldehyde intermediates *in situ*. These intermediates subsequently underwent  $\text{Yb(III)}$ -catalyzed sequential triazole reactions with 4-amino-1-methyl-3-propyl-1H-pyrazole-5-carboxamide **168**, affording the target compounds in moderate-to-good yields. This strategy demonstrated a broad tolerance for different substituents on both the terminal alkynes (OMe, OEt, Me, Et, *n*Pr, *n*Bu, and Cl) and the aromatic aldehydes (OMe, F,  $\text{NO}_2$ , Me, and Cl). The approach was further applied to synthesize 6-aryl-8H-isoquinolino[1,2-*b*]quinazolin-8-one derivatives. Subsequently, the prepared compounds were evaluated through molecular docking at the MtbCM binding site (PDB 2FP2). Based on the favorable docking outcomes, the researchers performed an ultrasound-assisted one-pot synthesis to produce 6-arylpyrazolo[4,3:4,5]pyrimido[2,1-*a*]isoquinolin-8(9H)-one derivatives **169** (Scheme 44).

Three derivatives, namely **169a–169c**, which exhibited strong *in silico* interactions with CM, demonstrated significant *in vitro* inhibition efficiencies (60–67%) at 10  $\mu\text{M}$ . SAR analysis showed that attaching an  $\text{NO}_2$  group to the C-2 position of the core structure significantly boosted the potency of the active species, while the introduction of OMe and F groups at the same position resulted in moderate and low activities, respectively. Aryl substituents, such as *p*-methoxyphenyl and *p*-chlorophenyl groups at the C-6 position, were beneficial for promoting the



Scheme 44 Ultrasound irradiation assisted one-pot synthesis of 6-arylpyrazolo[4,3:4,5]pyrimido[2,1-*a*]isoquinolin-8(9H)-ones **169**.



antitubercular activity, in contrast to *p*-alkoxy and *p*-alkyl phenyl groups, which were less effective. Compound **169c** demonstrated a promising antitubercular potential in preliminary evaluations, supported by its MtbCM inhibitory activity, favorable docking results, and predictive absorption, distribution, metabolism, and excretion (ADME) properties.

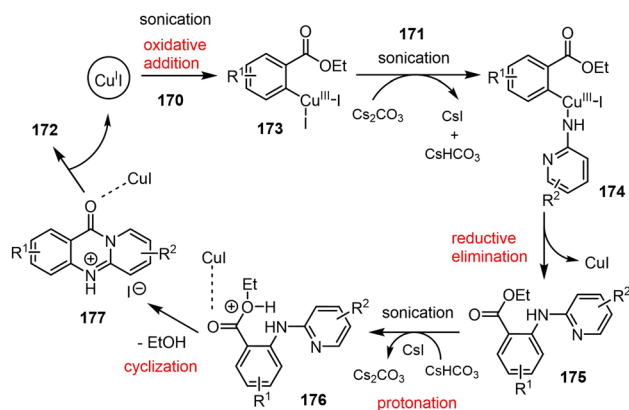
## 8. N-heterocycles with antiviral activities

N-heterocycles are a cornerstone in antiviral research due to their structural variety and significant biological activities. These nitrogen-containing rings interfere with viral propagation, enzyme activities, and entrance into host cells. At present, they continue to inspire innovative treatments against prevalent and emerging viruses, and are present in many licensed medications.<sup>119,120</sup>

### 8.1 Sonochemical synthesis of antiviral agents

**8.1.1 Quinazoline.** Matta *et al.* reported a novel synthetic strategy for the preparation of 11*H*-pyrido[2,1-*b*]quinazolin-11-one derivatives **172** (Scheme 45). Their route involved a CuI-catalyzed Ullmann–Goldberg coupling followed by a one-pot cyclization reaction under ultrasonic irradiation, affording the target products in moderate-to-good yields. Utilizing 2-iodobenzoate ester **170** in combination with 2-aminopyridine **171**, quinolin-2-amine, or thiazol-2-amine also led to successful formation of the desired compounds. Additionally, an *in silico* study was conducted to evaluate the interaction of these derivatives with the SARS-CoV-2 RNA-dependent RNA polymerase (RdRp).<sup>121</sup>

This copper-catalyzed, ultrasound-assisted reaction was initiated by the oxidative addition of CuI to the 2-iodobenzoate ester **170**, forming an intermediate **173** that reacts with 2-aminopyridine **171** to give a Cu-amidate complex **174**. Reductive



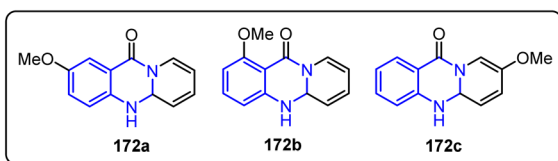
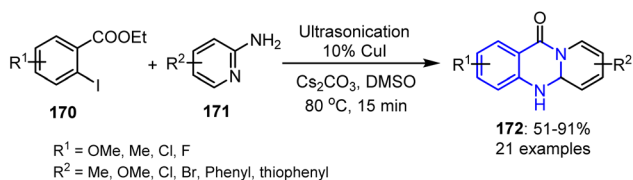
Scheme 46 Plausible mechanism for the sonochemical synthesis of 11*H*-pyrido[2,1-*b*]quinazolin-11-one derivatives **172**.

elimination subsequently yields a key intermediate **175**, which undergoes intramolecular cyclization *via* ester activation, forming 11*H*-pyrido[2,1-*b*]quinazolin-11-one **172**. Alternatively, CuI may initially bind to 2-aminopyridine before coupling, thereby generating the same product (Scheme 46).

Molecular docking studies targeting SARS-CoV-2 RdRp (PDB ID 7AAP) revealed that compounds **172a** and **172c** exhibited similar interaction profiles, while **172b** showed a binding efficiency that was nearly equivalent to those of favipiravir and remdesivir. Specifically, **172a** formed two hydrogen bonds, namely between its methoxy (OMe) group and THR556, and between its N-5 atom and SER682. Additionally, compound **172b** established hydrogen bonds between its OMe group and ARG624, and between its carbonyl (C=O) group and THR556. Compound **172c**, which demonstrated the most favorable binding energy, formed hydrogen bonds between its OMe group and THR556 and ARG624, and also between its N-5 atom and SER682. Pharmacokinetic evaluations indicated that all three compounds possessed favorable ADME properties, with the exception of their blood–brain barrier permeabilities. The work of Matta *et al.* therefore not only provides a CuI-catalyzed, ultrasound-assisted route to 11*H*-pyrido[2,1-*b*]quinazolin-11-one derivatives, but it also underscores the potential of these compounds for use as promising SARS-CoV-2 RdRp inhibitors.

**8.1.2 Isoquinoline.** Daliparthi *et al.* reported the synthesis of 1-aminoisoquinolines **180** under sonochemical conditions by treating 1-chloroisoquinoline **178** with different amines **179** in the presence of Cs<sub>2</sub>CO<sub>3</sub> and DMSO (Scheme 47).<sup>122</sup> This reaction began with an ultrasound-assisted nucleophilic attack by amine **179** on the chlorine-bearing C-1 atom of aromatic reactant **178**, forming a resonance-stabilized intermediate **181**. Ultrasonic irradiation facilitated both the nucleophilic substitution and the subsequent elimination of HCl from **181**, which restored aromaticity and efficiently yielded the final product **180**.

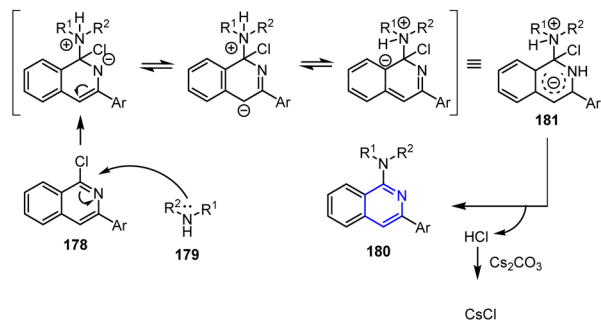
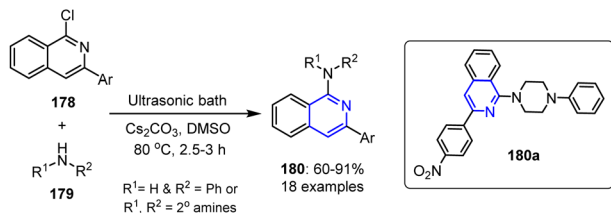
The same group further explored the antiviral potential of 1-aminoisoquinoline derivatives against the NS5 protein of the dengue virus (DENV) through *in silico* docking studies. Since the MTase domain of the NS5 protein is involved in RNA capping and the RdRp domain plays a key role in viral replication, both



Method	Temp	Duration	Yield
Conventional heating	80°C	60 min	46%
Ultrasonication	80°C	15 min	91%

Scheme 45 Copper-catalyzed one-pot synthesis of 11*H*-pyrido[2,1-*b*]quinazolin-11-ones **172** facilitated by ultrasonic irradiation.





Scheme 47 Sonochemical synthesis of 1-aminoisoquinoline derivatives **180** through the reaction of 1-chloroisoquinoline **178** with appropriate amines **179**.

were targeted during their work. Docking studies with the RdRp domain (PDB 5I3Q) revealed that compound **180a** forms strong hydrogen bonds with the GLN802, LEU511, and HIS512 residues through its NO<sub>2</sub> group. Similarly, docking into the DENV3 MTase domain (PDB 5EHG) showed that the same compound formed three hydrogen bond interactions with the GLY86, TRP87, and SER56 residues, highlighting its promising antiviral potential.

## 9. Conclusions

In conclusion, although non-conventional synthetic techniques, such as microwave- and ultrasound-assisted procedures have numerous advantages, they also exhibit various limitations. Specifically, the requirement for specialized equipment, which may raise initial costs and necessitate technical expertise, is one of the main disadvantages. These techniques may also be less scalable, thereby rendering them less appropriate for use in large-scale industrial manufacturing. An inconsistent product quality may also result from the possibility of hot patches or uneven heating during microwave synthesis. Furthermore, ultrasonic bath reactions frequently suffer from poor reproducibilities due to differences in the bath layouts and a lack of standardized control over the ultrasonic power. Despite these challenges, there are numerous benefits to non-conventional approaches. For example, these methods greatly shorten the reaction times, increase yields, and lead to improved selectivities compared with those achieved using conventional synthetic methods. Moreover, through the use of reduced solvent volumes and lower extents of energy consumption, they also provide more environmentally friendly and energy-efficient alternatives. Consequently, non-conventional routes tend to be more efficient, sustainable, and reproducible than traditional

approaches, which is particularly significant for the rapid and effective synthesis of bioactive molecules.

In this review, the preparation of a range of N-heterocyclic compounds using non-conventional synthetic techniques was examined. The findings of this review suggest that such approaches offer numerous advantages, including higher yields, a reduced environmental impact, and enhanced selectivities. The biological activities of the synthesized N-heterocyclic compounds were subsequently evaluated, revealing noteworthy potential in various applications due to their antimicrobial, anticancer, anti-inflammatory, and antiviral activities. Microwave-assisted routes yielded compounds with enhanced potencies and selectivities, highlighting their potential for use as drug candidates in diverse therapeutic applications.

Overall, this review highlights the significance of non-traditional synthetic approaches as effective and sustainable strategies for the production of biologically active N-heterocyclic compounds. The presented results pave the way for new opportunities in drug discovery and in the development of novel pharmaceuticals. Nonetheless, further work in this field should concentrate on enhancing the reproducibility, including through the use of continuous-flow and extrusion technologies, along with the integration of artificial intelligence and *in situ* monitoring. These techniques will be expected to provide greener, faster, and more efficient alternatives to traditional processes, thereby playing an important role in sustainable chemical production.

## 10. Future development on non-conventional synthesis techniques

### 10.1 Microwave assisted synthesis (MAOS)

Anticipated advancements in microwave-assisted synthesis are likely to transition from fixed-frequency setups to variable-frequency and tailored field irradiation, facilitating more precise control over energy distribution. The design of reactors will emphasize the development of rational catalyst supports, microwave-transparent flow cells, and hybrid technologies that integrate microwave energy with induction heating, ultrasound, or photo redox activation. Furthermore, the incorporation of digital twin models is expected to enable predictive design and reliable scale-up, thereby mitigating the current challenges of non-uniform heating and poor reproducibility.

### 10.2 Sonochemical synthesis

The future of sonochemistry will predominantly focus on the utilization of multi-frequency, pulsed, and chirped ultrasonic waves to achieve programmable cavitation. This approach will facilitate precise control over bubble collapse and radical synthesis. Additionally, it is anticipated that hybrid systems, such as sonophotocatalysis and sonoelectrochemistry, will become prevalent for complex oxidation processes and selective reactions. These systems will be enhanced by specially engineered reactor surfaces that concentrate cavitation effects at catalyst interfaces.



### 10.3 Mechanochemical synthesis

Mechanochemistry is expected to progress beyond traditional ball milling techniques, advancing towards resonant acoustic mixing and continuous, recipe-controlled extrusion. These developments will offer scalable methods for the preparation of complex materials and active pharmaceutical ingredients (APIs). The integration of *operando* multi-modal monitoring technologies, such as torque measurement, acoustic sensors, and Raman spectroscopy, will facilitate real-time management and control over polymorph selectivity. Furthermore, mechano-biocatalysis and biomass upgrading present promising opportunities for sustainable processes within green chemistry. Specifically designed tribo- and piezo catalysts are anticipated to enhance the utilization of mechanical energy.

The progression of these non-conventional methodologies will depend on the establishment of standardized process analytical technologies (PAT), the integration of real-time sustainability metrics and life-cycle assessments, and the implementation of unified reporting protocols to ensure reproducibility. Artificial intelligence and machine learning are anticipated to play a pivotal role in optimizing reaction conditions by correlating waveform, field, or mechanical inputs with desired outcomes. Additionally, the development of modular hybrid systems that integrate mechanical, acoustic, microwave, photochemical, and electrochemical methodologies will enhance the synthetic repertoire. Collectively, these innovations will facilitate reproducible, scalable, and environmentally sustainable chemical transformations that exceed the limitations of traditional synthetic strategies.

### Author contributions

N. S.: writing—original draft; K. S.: writing—original draft; K. K.: resources, writing—original draft; M. D. K.: writing—original draft; T. D.: conceptualization, funding acquisition, resources, supervision, writing—review and editing; F. V. S.: conceptualization, project administration, supervision, writing—review and editing.

### Conflicts of interest

We declare we have no competing interests.

### Data availability

No new data was created or analyzed during this study. Therefore, data sharing is not applicable.

### Acknowledgements

N. S., K. S., and F. V. S. acknowledge the support from Vellore Institute of Technology, Chennai. T. D. and K. K. acknowledge support from JSPS KAKENHI grant number 23K04827 (K. K.) and JST CREST grant number JPMJCR20R1 and the Ritsumeikan Global Innovation Research Organization (R-GIRO) project.

### References

- G. Meera, K. R. Rohit, S. Saranya and G. Anilkumar, *RSC Adv.*, 2020, **10**, 36031–36041.
- R. Tandon, I. Singh, V. Luxami, N. Tandon and K. Paul, *Chem. Rec.*, 2019, **19**, 362–393.
- Y. J. Wu, *Prog. Heterocycl. Chem.*, 2012, **24**, 1–53.
- F. Bassyouni, M. Tarek, A. Salama, B. Ibrahim, S. S. El Dine, N. Yassin, A. Hassanein, M. Moharam and M. Abdel-Rehim, *Molecules*, 2021, **26**, 2370.
- D. Matiadis and M. Sagnou, *Int. J. Mol. Sci.*, 2020, **21**, 5507.
- T. D. Montgomery and V. H. Rawal, *Org. Lett.*, 2016, **18**, 740–743.
- T. Liu and H. Fu, *Synthesis*, 2012, **44**, 2805–2824.
- P. Gandeepan and C. H. Cheng, *Chem.-Asian J.*, 2016, **11**, 448–460.
- A. Nandakumar, S. P. Midya, V. G. Landge and E. Balaraman, *Angew. Chem., Int. Ed.*, 2015, **54**, 11022–11034.
- P. B. Kole, K. Sakthivel, S. J. Armaković, S. Armaković, M. Iqbal, F. V. Singh and S. P. Kollur, *RSC Adv.*, 2024, **14**, 16960–16970.
- A. Dhakshinamoorthy and H. Garcia, *Chem. Soc. Rev.*, 2014, **43**, 5750–5765.
- K. Sakthivel, S. Niharan and F. V. Singh, *J. Organomet. Chem.*, 2024, 123290.
- N. T. Patil and Y. Yamamoto, *Chem. Rev.*, 2008, **108**, 3395–3442.
- A. Goel, N. Agarwal, F. V. Singh, A. Sharon, P. Tiwari, M. Dixit, R. Pratap, A. K. Srivastava, P. R. Maulik and V. J. Ram, *Bioorg. Med. Chem. Lett.*, 2004, **14**, 1089–1092.
- K. Sakthivel, P. B. Kole, R. Mangain and F. V. Singh, *Curr. Org. Chem.*, 2022, **26**, 1917–1934.
- S. E. Shetgaonkar, S. P. Kollur, R. R. Pillai, K. Thangavel, S. J. Armaković, S. Armaković, C. Shivamallu, R. G. Amachawadi, A. Syed, A. M. Elgorban and A. H. Bahkali, *Symmetry*, 2021, **13**, 1619.
- F. V. Singh, R. Kumar, A. Sharon, C. K. Broder, J. A. Howard, A. Goel and P. R. Maulik, *J. Mol. Struct.*, 2006, **782**, 55–59.
- K. Sakthivel, R. J. Gana, T. Shoji, N. Takenaga, T. Dohi and F. V. Singh, *Front. Chem.*, 2023, **11**, 1217744.
- M. Inoue, *Mater. Eng.*, 2005, **28**, 21.
- S. Majee, Shilpa, M. Sarav, B. K. Banik and D. Ray, *Pharmaceuticals*, 2023, **16**, 873.
- A. Das, D. Ray, M. W. Ashraf and B. K. Banik, *Curr. Top. Med. Chem.*, 2024, **24**, 19.
- R. Javahershenas, A. Makarem and K. D. Klika, *RSC Adv.*, 2024, **14**, 5547–5565.
- G. Tiwari, A. Khanna, V. K. Mishra and R. Sagar, *RSC Adv.*, 2023, **13**, 32858–32892.
- A. Adhikari, S. Bhakta and T. Ghosh, *Tetrahedron*, 2022, **126**, 133085.
- Y. V. D. Nageswar, K. Ramesh and K. Rakhi, in *Non-Conventional Synthesis*, 2024, ch. 4, pp. 95–128.
- O. Kamble, R. Chatterjee, R. Dandela and S. Shinde, *Tetrahedron*, 2022, **120**, 132893.



- 27 N. Kaur, *Mini-Rev. Org. Chem.*, 2019, **16**, 481–503.
- 28 S. K. Wahan, G. Bhargava and P. A. Chawla, *Curr. Org. Chem.*, 2023, **27**, 1010–1019.
- 29 J. F. Reynes, F. Leon and F. García, *ACS Org. Inorg. Au*, 2024, **4**, 432–470.
- 30 M. M. Li, X. Chen, Y. Deng and J. Lu, *RSC Adv.*, 2021, **11**, 38060–38078.
- 31 J. Akhtar, A. A. Khan, Z. Ali, R. Haider and M. S. Yar, *Eur. J. Med. Chem.*, 2017, **125**, 143–189.
- 32 B. M. Nugent, A. M. Buysse, M. R. Loso, J. M. Babcock, T. C. Johnson, M. P. Oliver, T. P. Martin, M. S. Ober, N. Breaux, A. Robinson and Y. Adelfinskaya, *Pest Manag. Sci.*, 2015, **71**, 928–936.
- 33 N. Kerru, L. Gummidi, S. Maddila, K. K. Gangu and S. B. Jonnalagadda, *Molecules*, 2020, **25**, 1909.
- 34 A. Omar, *Al-Azhar J. Pharm. Sci.*, 2020, **62**, 39–54.
- 35 A. R. Katritzky, *Adv. Heterocycl. Chem.*, Academic Press, 1997.
- 36 R. Mamgain, N. Sivaraj and F. V. Singh, *Adv. Heterocycl. Chem.*, 2025, **146**, 87–150.
- 37 K. Kranjc and M. Kocevar, *Curr. Org. Chem.*, 2010, **14**, 1050–1074.
- 38 V. Polshettiwar and R. S. Varma, *Acc. Chem. Res.*, 2008, **41**, 629–639.
- 39 P. Lidström, J. Tierney, B. Wathey and J. Westman, *Tetrahedron*, 2001, **57**, 9225–9283.
- 40 A. Daştan, A. Kulkarni and B. Török, *Green Chem.*, 2012, **14**, 17–37.
- 41 M. Henary, C. Kananda, L. Rotolo, B. Savino, E. A. Owens and G. Cravotto, *RSC Adv.*, 2020, **10**, 14170–14197.
- 42 J. Jacob, *Int. J. Chem.*, 2012, **4**, 29.
- 43 S. Nain, R. Singh and S. Ravichandran, *Adv. J. Chem., Sect. A*, 2019, **2**, 94–104.
- 44 B. L. Hayes, *Aldrichim. Acta*, 2004, **37**, 66–77.
- 45 K. W. Wagner, *Arch. Elektrotechnik*, 1914, **2**, 371–387.
- 46 V. Polshettiwar and R. S. Varma, *Acc. Chem. Res.*, 2008, **41**, 629–639.
- 47 V. Polshettiwar and R. S. Varma, *Chem. Soc. Rev.*, 2008, **37**, 1546–1557.
- 48 L. H. Lu, S. J. Zhou, M. Sun, J. L. Chen, W. Xia, X. Yu, X. Xu and W. M. He, *ACS Sustain. Chem. Eng.*, 2018, **7**, 1574–1579.
- 49 B. Banerjee, *Ultrason. Sonochem.*, 2017, **35**, 15–35.
- 50 Y. Jiang, X. Chen, L. Qu, J. Wang, J. Yuan, S. Chen, X. Li and C. Qu, *Ultrason. Sonochem.*, 2011, **18**, 527–533.
- 51 N. M. A. El-Rahman, T. S. Saleh and M. F. Mady, *Ultrason. Sonochem.*, 2009, **16**, 70–74.
- 52 W. Gao, J. Liu, Y. Jiang and Y. Li, *Beilstein J. Org. Chem.*, 2011, **7**, 210–217.
- 53 A. Bazgir, S. Ahadi, R. Ghahremanzadeh, H. R. Khavasi and P. Mirzaei, *Ultrason. Sonochem.*, 2010, **17**, 447–452.
- 54 R. Cella and H. A. Stefani, *Tetrahedron*, 2009, **65**, 2619–2641.
- 55 G. Cravotto and P. Cintas, *Chem. Soc. Rev.*, 2006, **35**, 180–196.
- 56 A. A. Belew and M. A. Assege, *Results Chem.*, 2025, **8**, 102438.
- 57 L. Peng, Y. Liu and D. Wei, *Acc. Mater. Res.*, 2025, **6**, 991–1005.
- 58 M. X. Li, H. Wang, S. W. Liang, M. Shao, X. He, Z. X. Wang and S. R. Zhu, *Cryst. Growth Des.*, 2009, **9**, 4626–4633.
- 59 Z. Fang, W. Yang, J. He, K. Ding, X. Wu, Q. Zhang, R. Yu and C. Lu, *CrystEngComm*, 2012, **14**, 4794–4800.
- 60 A. Q. Khan and S. Uddin, *Asian Pac. J. Cancer Prev.*, 2021, **22**(S1), 1–2.
- 61 C. Kim and B. Kim, *Nutrients*, 2018, **10**, 1021.
- 62 T. K. Chakraborty and S. Das, *Curr. Med. Chem.: Anti-Cancer Agents*, 2001, **1**, 131–149.
- 63 S. Manta, N. Tzioumaki, N. Kollatos, P. Andrea, M. Margaritouli, A. Panagiotopoulou, I. Papanastasiou, C. Mitsos, A. Tsotinis, D. Schols and D. Komiotis, *Curr. Microwave Chem.*, 2018, **5**, 23–31.
- 64 F. Shi, X. N. Zeng, G. Zhang, N. Ma, B. Jiang and S. Tu, *Bioorg. Med. Chem. Lett.*, 2011, **21**, 7119–7123.
- 65 T. Patel, R. Gaikwad, K. Jain, R. Ganesh, Y. Bobde, B. Ghosh, K. Das and S. Gayen, *ChemistrySelect*, 2019, **4**, 4478–4482.
- 66 S. Shroff, I. Baitharu, S. A. Mir, B. Nayak and A. K. Behera, *Results Chem.*, 2022, **4**, 100647.
- 67 X. J. Song, Y. Shao and X. G. Dong, *Chin. Chem. Lett.*, 2011, **22**, 1036–1038.
- 68 L. Li, J. Q. Cao, H. M. Liu, Q. Wu, Q. H. Pan, Z. P. Zeng, Y. T. Lan, Y. M. Li, W. J. Mei, X. C. Wang and W. J. Zheng, *Molecules*, 2017, **22**, 829.
- 69 V. N. M. de Oliveira, F. G. dos Santos, V. P. G. Ferreira, H. M. Araújo, C. do Ó Pessoa, R. Nicolete and R. N. de Oliveira, *Synth. Commun.*, 2018, **48**, 2522–2532.
- 70 H. R. Babu, M. Ravinder and S. Narsimha, *Asian J. Pharm. Pharmacol.*, 2019, **5**, 1202–1210.
- 71 A. I. Siutkina, S. Kalinina, R. Liu, L. H. Heitman, A. Junker, C. G. Daniliuc and D. V. Kalinin, *ACS Omega*, 2023, **8**, 14097–14112.
- 72 L. Imberg, S. Platte, C. Erbacher, C. G. Daniliuc, S. A. Kalinina, W. Dörner, A. Poso, U. Karst and D. V. Kalinin, *ACS Pharmacol. Transl. Sci.*, 2022, **5**, 1318–1347.
- 73 C. Dunker, L. Imberg, A. I. Siutkina, C. Erbacher, C. G. Daniliuc, U. Karst and D. V. Kalinin, *Pharmaceuticals*, 2022, **15**, 1340.
- 74 S. Platte, M. Korff, L. Imberg, I. Balicoglu, C. Erbacher, J. M. Will, C. G. Daniliuc, U. Karst and D. V. Kalinin, *ChemMedChem*, 2021, **16**, 3672–3690.
- 75 M. Korff, L. Imberg, J. M. Will, N. Bückreiß, S. A. Kalinina, B. M. Wenzel, G. A. Kastner, C. G. Daniliuc, M. Barth, R. A. Ovsepyan and K. R. Butov, *J. Med. Chem.*, 2020, **63**, 13159–13186.
- 76 S. Hati, S. Tripathy, P. K. Dutta, R. Agarwal, R. Srinivasan, A. Singh, S. Singh and S. Sen, *Sci. Rep.*, 2016, **6**, 32213.
- 77 T. Arasakumar, S. Mathusalini, A. Ata, R. Shankar, S. Gopalan, K. Lakshmi, P. Sakthivel and P. S. Mohan, *Mol. Divers.*, 2017, **21**, 37–52.
- 78 P. Saraswat, G. Jeyabalan, M. Z. Hassan, M. U. Rahman and N. K. Nyola, *Synth. Commun.*, 2016, **46**, 1643–1664.
- 79 D. F. Katowah, H. M. Hassaneen and T. A. Farghaly, *Arab. J. Chem.*, 2022, **15**, 103930.
- 80 S. Adapa, U. S. Kodali, A. K. Taneja, V. Bandaru, B. T. Mandava, B. Balakrishna, B. T. Mandava,



- N. Panigrahi, M. V. Rao and M. Pal, *Tetrahedron Lett.*, 2023, **131**, 154784.
- 81 G. V. Rao, A. K. Taneja, M. B. Tej, K. N. Sri, S. Vijayavardhini, S. Dandamudi, S. V. Chinnamaneni, R. Kapavarapu, M. V. Rao and M. Pal, *J. Mol. Struct.*, 2023, **1292**, 136239.
- 82 G. V. Rao, S. Dandamudi, M. B. Tej, S. V. Chinnamaneni, P. C. Vasireddy, R. Kapavarapu, M. V. Rao and M. Pal, *Tetrahedron Lett.*, 2023, **126**, 154659.
- 83 M. S. Ibrahim, B. Farag, J. Y. Al-Humaidi, M. E. Zaki, M. Fathalla and S. M. Gomha, *Molecules*, 2023, **28**, 3869.
- 84 B. Chakraborty and E. Chettri, *Results Chem.*, 2020, **2**, 100037.
- 85 B. Filipić, D. Ušjak, M. H. Rambaher, S. Oljatic and M. T. Milenković, *Front. Cell. Infect. Microbiol.*, 2024, **14**, 1370062.
- 86 B. Zhang, *Eur. J. Med. Chem.*, 2019, **168**, 357–372.
- 87 N. Baral, D. R. Mishra, N. P. Mishra, S. Mohapatra, B. P. Raiguru, P. Panda, S. Nayak, M. Nayak and P. S. Kumar, *J. Heterocycl. Chem.*, 2020, **57**, 575–589.
- 88 N. Baral, S. Mohapatra, B. P. Raiguru, N. P. Mishra, P. Panda, S. Nayak, S. K. Pandey, P. S. Kumar and C. R. Sahoo, *J. Heterocycl. Chem.*, 2019, **56**, 552–565.
- 89 D. Ashok, G. Thara, B. K. Kumar, G. Srinivas, D. Ravinder, T. Vishnu, M. Sarasija and B. Sushmitha, *RSC Adv.*, 2023, **13**, 25–40.
- 90 G. Surineni, P. Yogeewari, D. Sriram and S. Kantevari, *Med. Chem. Res.*, 2015, **24**, 1298–1309.
- 91 S. Kumar, A. Patel and N. Ahmed, *RSC Adv.*, 2015, **5**, 93067–93080.
- 92 M. Pradeep, M. Vishnuvardhan and T. Gangadhar, *Chem. Data Collect.*, 2023, **46**, 101020.
- 93 M. A. El-Borai, H. F. Rizk, M. F. Abd-Aal and I. Y. El-Deeb, *Eur. J. Med. Chem.*, 2012, **48**, 92–96.
- 94 N. R. Darekar, B. K. Karale, H. N. Akolkar and A. S. Burungale, *Russ. J. Gen. Chem.*, 2020, **90**, 1721–1726.
- 95 X. L. Hu, Z. Xu, M. L. Liu, L. S. Feng and G. D. Zhang, *Curr. Top. Med. Chem.*, 2017, **17**, 3219–3231.
- 96 S. Chauhan, V. Verma, D. Kumar, R. Gupta, S. Gupta, A. Bajaj, A. Kumar and M. Parshad, *Synth. Commun.*, 2022, **52**, 898–911.
- 97 S. K. J. Shaikh, R. R. Kamble, P. K. Bayannavar, S. M. Somagond and S. D. Joshi, *J. Mol. Struct.*, 2020, **1203**, 127445.
- 98 L. J. Min, Y. X. Shi, H. K. Wu, Z. H. Sun, X. H. Liu, B. J. Li and Y. G. Zhang, *Appl. Sci.*, 2015, **5**, 1211–1220.
- 99 N. J. Parmar, B. R. Pansuriya, H. A. Barad, R. Kant and V. K. Gupta, *Bioorg. Med. Chem. Lett.*, 2012, **22**, 4075–4079.
- 100 P. Acosta, E. Butassi, B. Insuasty, A. Ortiz, R. Abonia, S. A. Zacchino and J. Quiroga, *Molecules*, 2015, **20**, 8499–8520.
- 101 J. Tang, J. Li, L. Zhang, S. Ma, D. Shi, Q. Zhang, L. Yang, X. Wang, X. Liu and C. Liu, *J. Heterocycl. Chem.*, 2012, **49**, 533–542.
- 102 D. Silva, M. Chioua, A. Samadi, M. C. Carreiras, M. L. Jimeno, E. Mendes, C. De Los Ríos, A. Romero, M. Villarroya, M. G. López and J. Marco-Contelles, *Eur. J. Med. Chem.*, 2011, **46**, 4676–4681.
- 103 A. K. Chhillar, P. Arya, C. Mukherjee, P. Kumar, Y. Yadav, A. K. Sharma, V. Yadav, J. Gupta, R. Dabur, H. N. Jha and A. C. Watterson, *Bioorg. Med. Chem. Lett.*, 2006, **14**, 973–981.
- 104 A. Goyal, S. Sharma and J. Gaba, *Indian J. Chem.*, 2017, **56**, 334.
- 105 S. Jaiswal, *J. Mod. Trends Sci. Technol.*, 2019, **5**, 36–39.
- 106 M. Asif, M. Imran and Abida, *Mini-Rev. Org. Chem.*, 2022, **19**, 166–172.
- 107 T. A. Farghaly, M. A. Abdallah and Z. A. Muhammad, *Molecules*, 2011, **16**, 10420–10432.
- 108 M. S. Kamel, A. Belal, M. O. Aboelez, E. K. Shokr, H. Abdel-Ghany, H. S. Mansour, A. M. Shawky and M. A. El-Remaily, *Molecules*, 2022, **27**, 2061.
- 109 V. Zaharia, A. Silvestru, N. Palibroda and C. R. Mogoşan, *Farmacía*, 2011, **59**, 624–635.
- 110 Z. Huang, X. Zhang, J. Li, L. Zhang, Y. Shen, R. Wang, Y. Zhang and Z. Mao, *Bioorg. Chem.*, 2025, **138**, 108200.
- 111 S. M. Sondhi, J. Singh, P. Roy, S. K. Agrawal and A. K. Saxena, *J. Med. Chem.*, 2011, **20**, 887–897.
- 112 K. Sharma, N. Khatik, A. R. Khandelwal, R. Meena, H. L. Singh, S. Khaturia and H. Sachdeva, *J. Organomet. Chem.*, 2024, **1011**, 123127.
- 113 B. Dwivedi, D. Bhardwaj and D. Choudhary, *ChemistrySelect*, 2024, **9**, e202403884.
- 114 A. Arumugam, R. Shanmugam, S. Munusamy, S. Muhammad, H. Algarni and M. Sekar, *ACS Omega*, 2023, **8**, 15168–15180.
- 115 A. Narayanswamy, D. Ramakrishna, P. R. Shekar, S. Rajendrachari and R. Sudhakar, *ACS Omega*, 2024, **9**, 13262–13273.
- 116 S. Sharma, P. K. Sharma, N. Kumar and R. Dudhe, *Biomed. Pharmacother.*, 2011, **65**, 244–251.
- 117 A. Andreani, M. Granaola, A. Leoni, A. Locatelli, R. Morigi and M. Rambaldi, *Eur. J. Med. Chem.*, 2001, **36**, 743–746.
- 118 V. R. Sangepu, K. K. Jain, R. D. Bhoomireddy, D. Sharma, R. Venkateshwarlu, R. Kapavarapu, R. Dandela and M. Pal, *J. Mol. Struct.*, 2023, **1278**, 134909.
- 119 G. Ahmad, M. Sohail, M. Bilal, N. Rasool, M. U. Qamar, C. Ciurea, L. G. Marceanu and C. Misarca, *Molecules*, 2024, **29**, 2232.
- 120 Kanupriya, R. K. Mittal, V. Sharma, T. Biswas and I. Mishra, *Med. Chem.*, 2024, **20**, 487–502.
- 121 M. Manikantha, K. Deepti, M. B. Tej, M. B. Tej, A. G. Reddy, R. Kapavarapu, D. K. Barange, M. B. Rao and M. Pal, *J. Mol. Struct.*, 2023, **1280**, 135044.
- 122 D. E. P. Rao, M. B. Tej, M. D. Raju, N. R. K. Reddy, M. B. Tej, C. Rajendiran, P. C. R. Vasireddy, R. Kapavarapu, P. Pal, M. V. B. Rao and M. Pal, *ChemistrySelect*, 2024, **9**, e202304384.

